TECHNICAL REPORT
IGE-345

Specifications and User Guide for NAP : module in DRAGON/DONJON VERSION5 (Pin Power Reconstruction module)

R. Chambon

Institut de génie nucléaire
Département de génie mécanique
École Polytechnique de Montréal
23 octobre 2014

Contents

1 Context

In order to better optimize the fuel energy efficiency in PWR, the burnup distribution has to be known as accurately as possible, ideally in each pin. Since full transport calculation on a entire core is not possible within reasonable time as required by operation needs, other methodologies have to be followed. The usual approach is to use the two steps method where transport calculations are performed at assembly level, and homogenized properties are generated to be used at the core level, by diffusion calculations in our case. The disadvantage of this methodology is mainly the loss of details at assembly and pin levels. The pin-by-pin power reconstruction (PPR) method can be used to get back those levels of details as accurately as possible in a small additional computing time frame compared to classical core calculations. This methodology can be seen as a de-homogenization technique for core calculations using arbitrarily homogenized fuel assembly geometries. It was presented originally by Fliscounakis et al [1] as the generalized pin-power reconstruction (GPPR). More details on the methodology and some improvements were also presented by Brosselard et al [2].

The pin-by-pin power reconstruction methodology has been programmed as a new module called `NAP:` in the neutronic codes DRAGON (transport) and DONJON (diffusion) version 5. With this module, the pin-by-pin power reconstruction would be facilitated and made available in an open-source environment. The `NAP:` module is based on a classical flux factorization approach initially proposed by Fliscounakis et al [1].

The computer code DRAGON is a lattice code designed around solution techniques of the neutron transport equation.[3] The DRAGON project results from an effort made at *École Polytechnique de Montréal* to rationalize and unify into a single code the different models and algorithms used in a lattice code. [4–7] One of the main concerns was to ensure that the structure of the code was such that the development and implementation of new calculation techniques would be facilitated. DRAGON is therefore a lattice cell code which is divided into many calculation modules linked together using the GAN generalized driver[8, 9]. These modules exchange informations only via well defined data structures.

Similarly, the computer code DONJON [10] is the core code designed around solution techniques of the neutron diffusion equation. The same approach was followed to program the DONJON code as for DRAGON : modules, defined data structures and the GAN generalized driver. The main interface between the two codes are the data structures used to store cross-sections. There are three types : CPO, FBMXSDB and MULTICOMPO. The major difference is that cross-sections may depend of the burnup only with the first type, whereas with the second and third type additional parameters can vary. The second type is dedicated to CANDU reactors calculations and the additional parameter types are fixed. The MULTICOMPO was then naturally selected for this application because additional parameters are defined by the user.

We will present in Section 2 the theory behind the pin power reconstruction including how reaction rates are conserved between assembly and core calculations and how flux continuity is ensured. In the same section, PPR theory will also be explained. Section 3 described the algorithm used the algorithm used in DRAGON and DONJON to perform the PPR. Then, the test cases used for validation are presented in Section 4 together with the numerical results analyzes. Section 5 presents the main changes in the DRAGON-DONJON code and introduces a set of procedures to be used for post-treatment with Octave. Finally, conclusions and recommendations are given in Section 6.

The implementation and the features of the new module `NAP:` are presented together in the user guide of DONJON [10].

2 Theorical background

The purpose of this project is to program the pin-power reconstruction in DRAGON and DONJON v.5. As we will see in the algorithm section, several steps are involved in the overall calculations and many options can be chosen. In this section, we will present the theory behind the three main steps :

- Homogenization and condensation requirements
- Normalization of the equivalence coefficients
- Pin-power reconstruction

2.1 Homogenization and condensation

In core calculations, the number of neutron energy groups and the spatial mesh are reduced to be able to perform fast computations of the flux / power distribution. Average properties are then required for each macro region and each macro group. To get this information, homogenization and condensation methods are used following the more detailed transport calculations at pin / assembly level. The main concern during this process is to preserve reaction rates, i.e. make sure that the number of reactions occurring in each macro region i and each macro group g is the same whereas it is computed at the core level or at the assembly level. The basic method is to compute the following quantities for each macro region i and each macro group g :

- $\phi^g_{i,ref}$, the reference flux which is equal to the volume weighted average of the original flux and the sum of all original energy groups :

$$\phi^g_{i,ref} = \frac{1}{V_i} \sum_{r \in V_i} \sum_{k \in g} \phi_{ref}(r,k) V_r$$

- ϕ^g_i, the macro calculation flux, generally obtained by solving the diffusion equation over macro regions and macro groups.
- $\Sigma^g_{i,ref}$, the cross-sections which are equal to the ratio of the integrated reaction rate divided by its integrated flux over the macro region and macro group :

$$\Sigma^g_{i,ref} = \frac{\sum\limits_{r \in V_i} \sum\limits_{k \in g} \Sigma^k_{ref}(r) \phi^k_{ref}(r) V_r}{\sum\limits_{r \in V_i} \sum_{k \in g} \phi^k_{ref}(r) V_r} = \frac{\sum\limits_{r \in V_i} \sum\limits_{k \in g} \Sigma^k_{ref}(r) \phi^k_{ref}(r) V_r}{\phi^g_{i,ref} V_i}$$

First, to simplify the notation, the upper-script g for macro energy group will be shown only at the first occurrence of each quantity. Then using these notations, it can easily be seen that the reaction rates for the reference calculations τ_{ref} and the macro calculations τ_{mc} may be different since the reference average flux and the macro flux have been computed with different configuration and methods :

$$\tau_{ref} = \Sigma_{i,ref}.\phi_{i,ref}.V_i \;\neq\; \Sigma_{i,ref}.\phi_i.V_i = \tau_{mc} \tag{2.1}$$

To simplify the notations, no subscript is used for the flux when it refers to the macro-calculations : $\phi_i = \phi_{i,\text{mc}}$ unless specified.

To overcome the mathematical problem of Eq. 2.1, a transport-diffusion equivalence theory is used. One available method is the super homogenization methodology proposed previously by Hébert in [14]. To guaranty the reaction rates conservation, macroscopic cross-sections have to be modified. They are multiplied by a factor λ^g_i (written as λ_i after) and the new value is defined by :

$$\Sigma_i = \lambda_i \Sigma_{i,ref}$$

The macro-reaction rate is then given by :

$$\tau_{mc} = \Sigma_i.\phi_i(\Sigma_i) = \lambda_i \Sigma_{i,ref}.\phi_i(\lambda_i \Sigma_{i,ref}) \tag{2.2}$$

Using Eq. 2.2 to have both reaction rates of Eq. 2.1 equal, λ_i has to be defined as follows :

$$\lambda_i = \frac{\phi_{i,ref}}{\phi_i(\lambda_i \Sigma_{i,ref})} \tag{2.3}$$

Since the diffusion flux distribution depends on the cross-sections, finding the set of λ_i factors that guaranties the same reaction rates is an iterative process.

2.2 Equivalence coefficients

In the transport-diffusion equivalence theory presented in the previous section, the set of coefficients $\{\lambda_i\}$ can be divided by any constant α^g (written as α after). This is based on the fact that in an infinite domain, if the cross-sections Σ_i are divided by a factor α ($\tilde{\Sigma}_i = \Sigma_i/\alpha$), the flux will be multiplied by the same factor $\tilde{\psi}(\Sigma_i/\alpha) = \alpha\psi(\Sigma_i)$, thus the reaction rate $\tilde{\tau}_{mc}$ remains the same as illustrated in the following equation :

$$\tilde{\tau}_{mc}(\tilde{\Sigma}_i) = \tilde{\Sigma}_i.\tilde{\phi}_i(\tilde{\Sigma}_i).V_i = \frac{\Sigma_i}{\alpha}.\tilde{\phi}_i(\frac{\Sigma_i}{\alpha})V_i = \frac{\Sigma_i}{\alpha}.\alpha\phi_i(\Sigma_i)V_i = \tau_{mc}(\Sigma_i)$$

Note that the factor α is different for each energy group, but is the same for all the macro-regions and all cross-section types. α can be seen as a normalization coefficient.

An other quantity is also defined : the SPH factors μ_i^g and the average SPH factor $\bar{\mu}^g$ (written as μ_i and $\bar{\mu}$ after) which are defined by :

$$\tilde{\phi}_i = \frac{\phi_i}{\mu_i}$$

where

$$\mu_i = \lambda_i/\alpha \tag{2.4}$$

and

$$\begin{aligned}
\bar{\phi}_{\mathrm{mc}}\bar{\mu} &= \overline{\tilde{\phi}} \\
&= \frac{1}{V_{tot}}\sum_i \frac{\phi_i V_i}{\mu_i} \\
&= \frac{1}{V_{tot}}\sum_i \frac{\phi_i V_i \lambda_i}{\alpha} \\
&= \frac{1}{\alpha.V_{tot}}\sum_i \phi_{i,\mathrm{ref}} V_i \\
&= \frac{\bar{\phi}_{\mathrm{ref}}}{\alpha}
\end{aligned}$$

then

$$\bar{\mu} = \frac{1}{\alpha}\frac{\bar{\phi}_{\mathrm{ref}}}{\bar{\phi}_{\mathrm{mc}}} \tag{2.5}$$

where $\bar{\phi}_{\mathrm{ref}}$ is the averaged volumic flux of the reference calculation and $\bar{\phi}_{\mathrm{mc}}$ is the averaged volumic flux of the macro-calculation on macro-group g.

2.2.1 Flux-Volume normalisation (STD)

One approach to normalize the $\{\lambda_i\}$ set is to make sure that the spatially integrated macro-calculation flux for each group is the same as in transport calculations. In this case, we can write :

$$\begin{aligned}\underbrace{\sum_i \phi_{i,ref} V_i}_{\bar{\phi}_{\text{ref}}.V_{tot}} &= \sum_i \phi_i(\tilde{\Sigma}_i) V_i \qquad (2.6)\\ &= \sum_i \alpha \phi_i(\Sigma_i) V_i \\ &= \alpha \underbrace{\sum_i \phi_i(\Sigma_i) V_i}_{\bar{\phi}_{\text{mc}}.V_{tot}} \\ \Rightarrow & \\ \alpha &= \frac{\bar{\phi}_{\text{ref}}}{\bar{\phi}_{\text{mc}}} \qquad (2.7)\end{aligned}$$

Then for the flux-volume normalization, the macro-fluxes in macro regions i in each macro-group are normalized using :

$$\tilde{\phi}_i = \phi_i \frac{\bar{\phi}_{\text{ref}}}{\bar{\phi}_{\text{mc}}} \qquad (2.8)$$

Using this definition and Eq. 2.5, the averaged SPH factor, $\bar{\mu}$, is equal to one. This normalization corresponds to the 'STD' option in the `SPH:` module of DRAGON.

The limitation of this approach is that the flux continuity is not guarantied between two different assemblies.

2.2.2 Selengut normalization (SELE_FD and SELE_EDF)

The idea of the Selengut approach is to guaranty the flux continuity between different assemblies. Note that the continuity is for 1D computations ; however, when applied to 2D, the methodology calculations provides good results in terms of continuity at assembly interfaces. The methodology consists in using a normalization factor α such that the flux at the assembly interface is equal to 1 (or any constant). On a practical point of view, the interface flux is approximated by the flux in a small volume surrounding the assembly, usually the water gap. For the Selengut normalization, the macro-fluxes in macro regions i in each macro-group are normalized using :

$$\tilde{\phi}_i = \phi_i \frac{\phi^{\text{gap}}_{\text{ref}}}{\bar{\phi}_{\text{mc}}} \qquad (2.9)$$

$$= \phi_i . \underbrace{\frac{\bar{\phi}_{\text{ref}}}{\bar{\phi}_{\text{mc}}}}_{\text{ratio reference/macro flux}} . \underbrace{\frac{\phi^{\text{gap}}_{\text{ref}}}{\bar{\phi}_{\text{ref}}}}_{\text{ratio boundary/average reference flux}} \qquad (2.10)$$

Using this definition and Eq. 2.5, the averaged SPH factor, $\bar{\mu}$, is equal to :

$$\bar{\mu} = \frac{\bar{\phi}_{\text{ref}}}{\phi^{\text{gap}}_{\text{ref}}}$$

This normalization corresponds to the 'SELE_FD' option in the `SPH:` module of DRAGON.

In the case of an heterogeneous homogenization, the ratio between the assembly-average and boundary reference flux may not be the most accurate one (second ratio in the RHS of Eq. 2.10). Instead of using

the average flux on the assembly, the average on the side (surrounding row of pin, i.e. mixtures, see Section A.1) can be used. Then for the heterogeneous Selengut normalization, the macro-fluxes in macro regions i in each macro-group are normalized using :

$$\tilde{\phi}_i = \phi_i . \underbrace{\frac{\bar{\phi}_{\text{ref}}}{\bar{\phi}_{\text{mc}}}}_{\text{ratio reference/macro flux}} . \underbrace{\frac{\phi_{\text{ref}}^{\text{gap}}}{\phi_{\text{ref}}^{\text{row}}}}_{\text{ratio boundary/side reference flux}} \tag{2.11}$$

Using this definition and Eq. 2.5, the averaged SPH factor, $\bar{\mu}$, is equal to :

$$\bar{\mu} = \frac{\phi_{\text{ref}}^{\text{row}}}{\phi_{\text{ref}}^{\text{gap}}} .$$

This normalization corresponds to the 'SELE_EDF' option in the `SPH:` module of DRAGON.

The limitation of this approach is that the flux continuity is guarantied between two different assemblies for the reference flux, i.e. transport calculations and not macro-calculations.

2.2.3 Selengut macro-calculation water gap normalization (SELE_MWG)

The Selengut macro-calculation water gap normalization is used to ensure the continuity of the reconstructed (i.e. diffusion) flux at the boundary. For this case, the macro flux is normalized as follows :

$$\tilde{\phi}_i = \phi_i \frac{\phi_{\text{ref}}^{\text{gap}}}{\phi_{\text{mc}}^{\text{surf}}} \tag{2.12}$$

$$= \phi_i . \underbrace{\frac{\bar{\phi}_{\text{ref}}}{\bar{\phi}_{\text{mc}}}}_{\text{ratio reference/macro average flux}} . \underbrace{\frac{\phi_{\text{ref}}^{\text{gap}}}{\phi_{\text{mc}}^{\text{surf}} \cdot \frac{\bar{\phi}_{\text{ref}}}{\bar{\phi}_{\text{mc}}}}}_{\text{ratio reference/macro side flux}} \tag{2.13}$$

Using this definition and Eq. 2.5, the averaged SPH factor, $\bar{\mu}$, is equal to :

$$\bar{\mu} = \frac{\bar{\phi}_{\text{ref}}\, \phi_{\text{mc}}^{\text{surf}}}{\bar{\phi}_{\text{mc}}\, \phi_{\text{ref}}^{\text{gap}}} .$$

This normalization corresponds to the 'SELE_MWG' option in the `SPH:` module of DRAGON.

Note that in the case of an homogeneous assembly, the Selengut macro-calculation water gap normalization is equivalent to the classical Selengut normalization since the diffusion flux is constant over the assembly : $\phi_{\text{mc}}^{\text{surf}} = \bar{\phi}_{\text{mc}}$.

2.3 Pin Power Reconstruction

2.3.1 Definition

As mention previously, the pin power reconstruction methodology can be seen as a de-homogenization technique for core calculations performed with arbitrarily homogenized fuel assembly geometries. The general idea is to look at the the detailed flux distribution ϕ_{det} in the core as the product of two contributions :

- the macro-flux provided by the macro-calculations, which represents the general shape at the core level, ϕ_{mc}
- the local flux provided by the transport calculations, which represents the 'ripple' shape at the assembly level, ϕ_{ref}

In order to keep consistency, the local flux is normalized and is referred as the shape factor. The reaction rate for each pin is then given by the following equation :

$$\tau_{i,p}^{Gen} = \tilde{\Sigma}_{p,ref} \times \phi_{i,p}(\tilde{\Sigma}_i) \times \underbrace{\frac{\phi_p^\infty(\Sigma_p)}{\phi_{i,p}^\infty(\Sigma_i)}}_{\text{shape factor}} .V_p \quad \text{with } 1 \leq i \leq M \text{ and } 1 \leq p \leq P \tag{2.14}$$

$$= \tilde{\Sigma}_{p,ref} \times \tilde{\phi}_{i,p}(\tilde{\Sigma}_i) \times \frac{\phi_{p,\text{ref}}}{\lambda_p \phi_{i,p}^\infty(\Sigma_i)} .V_p \tag{2.15}$$

where the subscripts i, p represent the projection of the macro calculations flux using general geometry on the pin-by-pin geometry.

As expected, the reaction rate is the product of the cross-section times the flux times the volume. However, since the flux is only the projection of the macro-calculation on each pin, it may differ from the reference flux. The shape factor introduced previously corrects this approximation. It also represents the ratio between the macro-calculation fluxes computed on a pin by pin and on a heterogeneous geometries in an infinite domain. Physically, this ratio can be seen as the relative error made when using a general geometry instead of the pin-by-pin geometry.

Using Eq. 2.3, the reference flux is introduced. The detailed flux is then clearly seen as the product of the macro-flux and normalized local flux (Eq. 2.15). The reaction rate equation is then the same as proposed by Brosselard et al [2]. Eq. 2.15 can be applied with any homogenization and was presented originally by Fliscounakis et al [1] as the generalized pin-power reconstruction (GPPR).

2.3.2 Computation

To perform the GPPR, the different components of Eq. 2.14 are obtained as follows :

- The cross-sections are recovered from the pin-by-pin wise homogenized data-structure.
- The macro-calculation flux is projected on each pin. Note that it is very important to interpolate the flux as well as we will see later.
- The components of the shape factor are pre-calculated.

Regarding the methodology used to compute the shape factor, two important notes have to be made. First, the macro-calculation flux has to be normalized ($\phi_{i,p}^\infty(\Sigma_i)$). The flux-volume normalization is used. The average reference and macro-calculation fluxes (over the assembly on one macro-energy group) are computed. Their ratio is used to normalize the projected macro-calculation flux on each pin. The results would be the same regardless of the SPH method used in the macro-calculation on the infinite domain. Indeed, we can write :

$$\begin{aligned}
\phi_{i,p}^\infty(\tilde{\Sigma}_i).\frac{\bar{\phi}_{\text{ref}}}{\bar{\phi}_{\text{mc}}^\infty(\{\tilde{\Sigma}_i\})} &= \phi_{i,p}^\infty(\frac{\Sigma_i}{\alpha}).\frac{\bar{\phi}_{\text{ref}}}{\bar{\phi}_{\text{mc}}^\infty(\{\frac{\Sigma_i}{\alpha}\})} \\
&= \alpha\phi_{i,p}^\infty(\Sigma_i).\frac{\bar{\phi}_{\text{ref}}}{\alpha\bar{\phi}_{\text{mc}}^\infty(\{\Sigma_i)\}} \\
&= \phi_{i,p}^\infty(\Sigma_i).\frac{\bar{\phi}_{\text{ref}}}{\bar{\phi}_{\text{mc}}^\infty(\{\Sigma_i)\})}
\end{aligned}$$

The second note concerns the choice of SPH normalization made in DRAGON. During the transport calculations, at the end of the SPH normalization, the cross-sections $\Sigma_{i,ref}$ are multiplied by the SPH factor $\mu_i = \lambda_i/\alpha$ and the reference flux $\phi_{i,\text{ref}}$ is divided by the same factor. The SPH corrected reference flux $\tilde{\phi}_{i,\text{ref}}$ can be defined as follows :

$$\begin{aligned}
\tilde{\phi}_{p,\text{ref}} &= \frac{\phi_{p,\text{ref}}}{\mu_p} \\
&= \frac{\phi_{p,\text{ref}}}{\lambda_p/\alpha}
\end{aligned}$$

Then, it is important to use the same SPH corrected cross-sections $\phi_{p,\text{ref}}$ for both the PPR and the normalization of $\phi^{\infty}_{i,p}$. Indeed when SPH corrected flux are used, the shape factor in the reaction rate equation (Eq. 2.14) can be written as follows :

$$\begin{aligned}
\frac{\tilde{\phi}_{p,\text{ref}}}{\phi^{\infty}_{i,p}(\Sigma_i).\frac{\bar{\tilde{\phi}}_{p,ref}}{\bar{\phi}^{\infty}_{\text{mc}}}} &= \frac{\phi_{p,\text{ref}}/(\lambda_p/\alpha)}{\phi^{\infty}_{i,p}(\Sigma_i).\frac{\bar{\phi}_{p,\text{ref}}/(\lambda_p/\alpha)}{\bar{\phi}^{\infty}_{\text{mc}}}} \\
&= \frac{\phi_{p,\text{ref}}/(\lambda_p/\alpha)}{\phi^{\infty}_{i,p}(\Sigma_i).\frac{\bar{\phi}_p.\alpha}{\bar{\phi}^{\infty}_{\text{mc}}}} \\
&= \frac{\phi_{p,\text{ref}}}{\frac{\lambda_p}{\alpha}.\phi^{\infty}_{i,p}(\Sigma_i).\frac{\bar{\phi}^{\infty}_{\text{mc}}.\alpha}{\bar{\phi}^{\infty}_{\text{mc}}}} \qquad (2.16) \\
&= \frac{\phi_{p,\text{ref}}}{\lambda_p\phi^{\infty}_{i,p}(\Sigma_i)} \qquad (2.17)
\end{aligned}$$

As Eq. 2.16 shows, the α factors can be removed only if the SPH correction is the same for both terms. Then, using the SPH corrected reference flux in the PPR takes into account the specific value of the SPH correction pin by pin, and using it in the normalization of the $\phi_{p,\text{ref}}$ takes into account the average value of these factors. Their ratio can then be seen as normalized SPH factor, i.e. their average equals to 1 which are the flux-volume SPH factors.

Note that homogenized cross-sections of macro-regions are not used to compute final reaction rates, but only used during the diffusion calculations. Then at the end of the transport calculation, two homogenizations are required : one to get the macro-region properties as usual for diffusion calculations, and one to get the properties homogenized on each pin. This means that two sets of cross-sections would have to be interpolated : one for the homogeneous (4x4) or heterogeneous (4x4*) based geometry and one for the pin wise geometry. The burnup distribution should match between the two geometries.

When an homogeneous homogenization is performed, the method is equivalent to the classical PPR because all projected flux are the same. Indeed, the diffusion flux is a constant in that case. Eq. 2.14 can be written as follows for an homogeneous Pin-Power Reconstruction (PPR) :

$$\tau^{Gen}_{i,p} = \tilde{\Sigma}_{p,ref} \times \phi_p(\tilde{\Sigma}) \times \frac{\phi_{p,\text{ref}}}{\lambda_p\phi^{\infty}_{mc}} = \tau^{Hom}_{p} \quad \text{with } 1 \leq p \leq P \qquad (2.18)$$

where the subscripts i are removed since the assembly is homogeneous.

3 Algorithm

This section presents the general algorithm. The procedure to perform pin-power reconstruction can be summarized in 3 steps as follows :

1. Follow the general procedure to compute a MULTICOMPO data-structure, and add the following features :.
   - Addition #1 : after each flux calculation, perform all homogenization types as needed by the `NAP:` module (depends on the chosen methodology for reaction rate calculation) : homogeneous, heterogeneous, pin by pin. It is recommended to save all cross-sections in different folder of the same MULTICOMPO data-structure.
   - Addition #2 : add the simplified unfolded geometry used for homogenization in the MULTICOMPO data-structure (through the `EDI:` module with `MGEO` keyword). See the user guide [10] for important note on the coarse geometry requirement.
2. Compute additional properties in diffusion theory for an assembly in infinite domain
   - Define a simple geometry in DONJON that is the same as the homogenized geometry in DRAGON (homogeneous, heterogeneous, pin by pin, ...).
   - For each burnup step in the MULTICOMPO data-structure, perform the following :
     (a) Compute the flux in an infinite domaine with the homogeneous or heterogeneous homogenized cross-sections
     (b) Project the flux on each pin (`NAP:` module) and store the results with the pin-by-pin homogenized cross-sections : L_COMPO/dir_pin/MIXTURES/CALCULATIONS/L_MICRO/MACROLIB/GROUP

   At this point, an enriched MULTICOMPO data-structure is obtained, and ready to be used for core calculations.
3. Core calculations
   (a) Compute the core flux distribution following the general procedure.
   - Warning : if heterogeneous cross-sections are used, the geometry definition has to match the discretization used for homogenization at assembly level in DRAGON. This can be done manually or automatically with the `NAP:` module.

   (b) Compute the corrected reaction rate using the additional properties in the enriched MULTICOMPO data-structure. Perform the pin power reconstruction if required by the chosen methodology.
   - **Note :** Reaction rates are saved in the MAP data-structure and can be printed in the output file for each assembly of the core.

The detailed algorithm is presented in Appendix (see Section A)

4 Validation

As previously mentioned, several clusters were simulated both in transport and diffusion theory to validate the GPPR. A total of 12 cluster configurations was used. They can be described as follows :

Assembly positions by type

C	B	C
B	A	B
C	B	C

Assembly types by case

Case	Burn-up (GWd/t)			Boron (ppm)
	A	B	C	
C1	0 (M)	0 (U)	20 (U)	1700
C2	20 (M)	10 (U)	60 (U)	715
C3	10 (M)	30 (M)	20 (U)	900
C4	20 (M)	50 (M)	0 (M)	1100
C5	20 (M)	20 (U)	20 (U)	1600
C6	0 (U)	30 (M)	30 (M)	715
C7	0 (M)	0 (M)	60 (U)	1100
C8	60 (M)	10 (U)	40 (M)	900
C9	12 (U)	12 (U)	12 (U)	2200
C10	0 (U)	36 (U)	12 (U)	1400
C11	20 (M)	0 (U)	40 (U)	2000
C12	12 (M)	12 (M)	12 (M)	2000

In order to develop an efficient and precise methodology for PPR, several parameters were looked as options. Three groups of tests were performed before converging to a recommended methodology :

1. Flux projection
2. Consistency of methodology for the computation of $\phi_{i,p}^{\infty}$ and $\phi_{i,p}$
3. Type (geometry) and methodology (Selengut) for homogenization and condensation.

4.1 Flux projection

Before presenting the results a very important note has to be made regarding the flux projection on the pins from the macro regions.

The purpose of the PPR is to be able to perform the calculations in a small additional time frame compared to classical diffusion calculations. In order to do so, the mesh used for the geometry per assembly remains relatively coarse (4x4 or 8x8), and does not fit a pin by pin description (17x17). However, most of the time the core flux is computed with advanced method such as Raviart-Thomas using finite elements with polynoms of order up to 3 to take into account the flux gradient within a single mesh. When the resulting average flux on each mesh computed with these advanced methods is projected on each pin ($\phi_{i,p}$), the approach is not precise enough for very heterogeneous assemblies or mixes of assemblies. In these cases, the flux gradient is very important as shown on LHS of Fig. 1 (configuration #8). In this figure, the black lines represent the geometry mesh (8x8*).The error between transport (reference) and diffusion in larger region clearly presents a gradient as shown by the white arrows. This results shows that the flux has to be re-interpolated within each mesh as during its calculation to capture the gradient before it is projected on each pin. It also shows that finite elements with too low polynomial order may lead to too large error. RHS of Fig. 1 shows results in the same configuration, with the same choices for homogenization and split but using the interpolated flux for both core and infinite domain diffusion flux. The interpolated flux is obtained using the Gauss interpolation technique which provides the integral of the flux over the pin plus surrounding water of one lattice pitch (plus water gap on border pins).

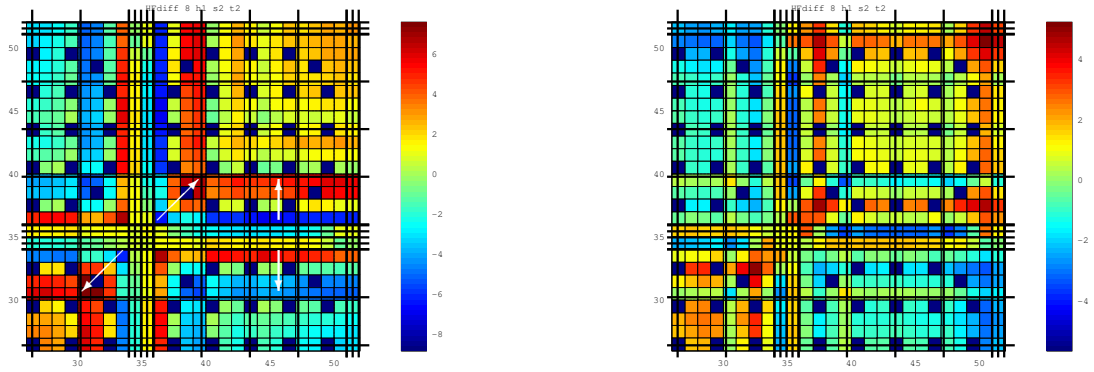

average flux interpolated polynomial flux

FIGURE 1 – **Relative error between transport and diffusion calculation ((D-T)/T (%)) using results of a RT2 calculation, case #8 - 8x8* - heterogeneous assembly 'het1'**

4.1.1 Flux projection validation

To verify the flux projection using the interpolation method. Two subroutines have been programmed in TRIVAC to interpolate flux computed with the Raviart-Thomas solver in 2D and 3D. Moreover, a new module `VAL:` has been programmed in TRIVAC to produce a data structure with interpolated flux. These data can be used in Octave procedures to plot the flux distribution. To test all these new capabilities before using them in the PPR module `NAP:`, we have simulated the benchmark IAEA2D as described in the DRAGON user guide [11]. The results presented on Fig. 2 show clearly that a higher order of Raviart-Thomas has to be used to get a proper representation of the real flux distribution in the core. Note that small discontinuity are still present between assembly even with higher polynomial order. This is an intrinsic feature of the Raviart-Thomas method which does not guaranty the continuity at interface when only the flux information is used (and not the current).

4.1.2 Flux projection results for clusters

To illustrate the efficiency of the interpolated compared to the average flux projection, the results for two configurations are presented on Fig. 3. Calculations were performed with a 4x4* geometry tracked using 'DUAL 2 3' option in `TRIVAT:` module. For each case, the first and the second lines correspond to the pin power and one group flux distribution respectively. The three columns show the results for transport, diffusion with Selengut without flux interpolation and diffusion with Selengut with flux interpolation . For diffusion calculations, the flux on the macro regions and on the pin are shown. As expected, the flux presents important discontinuity when the interpolation is not done. The more heterogeneous the assemblies are (case #8), the more the interpolation is relevant. Indeed, the range of error decreases from 18% to 9% for case #5 and from 23% to 10% for case #8.

4.2 Consistency of geometry and tracking

An attempt to simplify the general procedure has been made by studying the requirement for consistency of methodology for the computation of $\phi_{i,p}^{\infty}$. Tab 1 present the results performed with an 'het1' type homogenization for cases #7 and #8. The first column represents the reference case where both diffusion flux are computed with the same options in terms of geometry mesh and Raviar-Thomas method polynomial order. The reference results are present in an italic font. The second column presents the results with the same options but no interpolation during the computation of $\phi_{i,p}^{\infty}$ is used. The results in

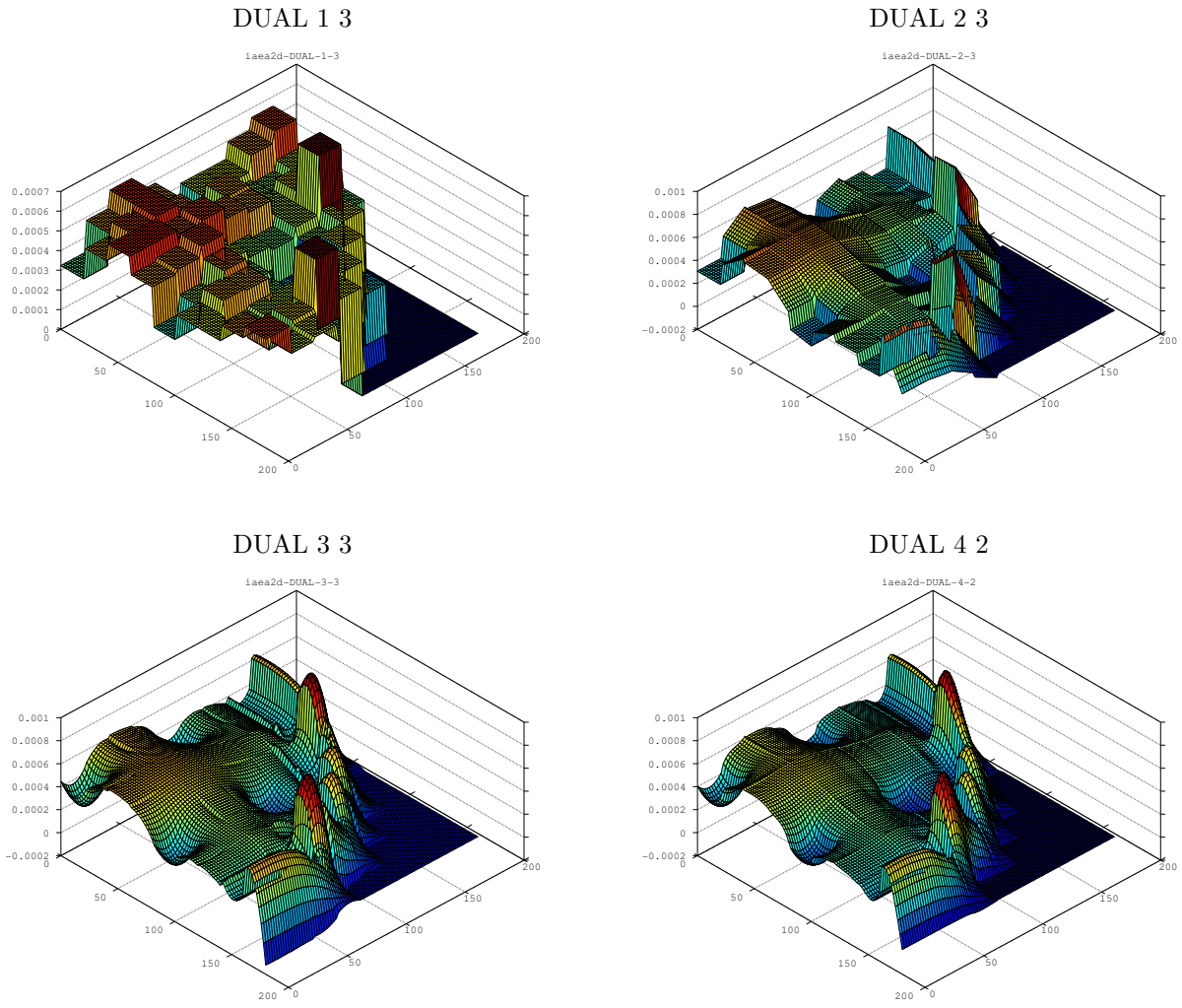

FIGURE 2 – Interpolated thermal flux distribution for IAEA2D benchmark, various order of Raviart-Thomas

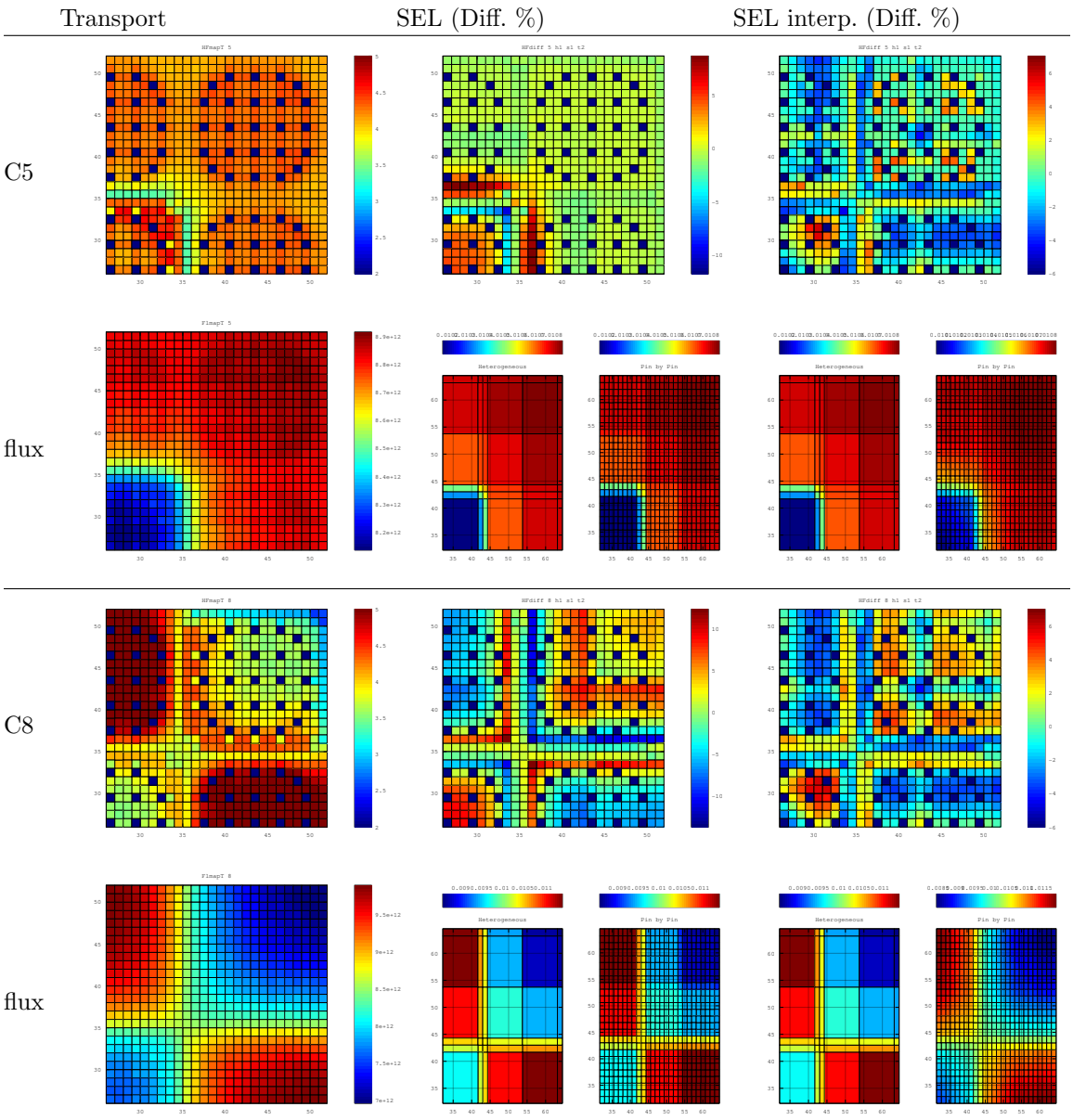

C5 has uniform burnup, C8 is completely heterogeneous.
Diffusion calculation performed with Selengut SELE_EDF option

FIGURE 3 – Transport vs diffusion (h1, s1, t2) pin power distribution of all clusters

this case confirm the first point regarding the mandatory to interpolate the flux at every step (specially for low polynomial order). The third and fourth columns provide results when the options for infinite domain diffusion flux are fixed at the lowest and highest precisions respectively : 4x4* and low order or 8x8* and high order. All results show that when the infinite domain and core calculations are not performed with consistent options the precision is reduced. Then, the results presented in Tab 1 show that diffusion calculations have to be performed with the same options for core ($\phi^{\infty}_{i,p}$) and infinite domain ($\phi_{i,p}$). The value presented in Tab 1 were computed using a different normalization of the $\phi^{\infty}_{i,p}$, and then differs slightly from those in appendix. However, the conclusions remain the same.

TABLE 1 – Relative error between reconstruction and transport calculations(%), comparison of different options to compute the PPR factor $\phi^{\infty}_{i,p}$

	Type : $\phi^{\infty}_{i,p}$ interp. ? ifx [+]	'het 1' 'yes' same as $\phi_{i,p}$			'het 1' 'not' same as $\phi_{i,p}$			'het 1' 'yes' fixed at 112 [+]			'het 1' 'yes' fixed at 123 [+]		
		min	max	std	min	max	std	min	max	std	min	max	std
		Heterogeneous 4x4*, SPH type 'SELE_EDF'											
C7	DUAL 2 3	*-4.09*	*6.73*	*2.04*	-7.99	7.40	2.77	*-4.09*	*6.73*	*2.04*	-5.86	7.70	2.35
	DUAL 3 3	*-4.61*	*5.12*	*1.70*	-4.22	5.85	2.22	-5.40	5.31	2.03	-4.29	5.17	1.84
C8	DUAL 2 3	*-4.38*	*5.82*	*2.43*	-6.70	6.51	2.81	*-4.38*	*5.82*	*2.43*	-5.40	6.63	2.77
	DUAL 3 3	*-3.30*	*5.46*	*1.87*	-4.32	5.38	1.93	-4.36	6.54	2.02	-3.54	5.91	1.95
		Heterogeneous 8x8*, SPH type 'SELE_EDF'											
C7	DUAL 2 3	*-4.05*	*5.25*	*1.87*	-8.53	7.05	2.85	-5.95	5.45	2.14	-4.85	5.50	1.98
	DUAL 3 3	*-3.95*	*5.08*	*1.69*	-4.07	6.81	2.22	-5.22	5.21	1.95	*-3.95*	*5.08*	*1.69*
C8	DUAL 2 3	*-3.10*	*3.93*	*1.66*	-7.06	5.93	2.27	-4.47	4.03	1.80	-3.72	4.50	1.76
	DUAL 3 3	*-3.11*	*3.23*	*1.63*	-3.38	5.94	1.69	-4.28	3.71	1.72	*-3.11*	*3.23*	*1.63*

[+] value of ifx 'XYZ' : X = type of homogeneization, Y = split level (1 for 4x4*, 2 for 8x8*), Z = DUAL value

4.3 Homogenization geometry and SPH method

The last point to analyze concerns the options of homogenization used to computed the cross-sections. Two parameters are looked at : the geometry with four choices as shown in Section A.3 and the SPH methodology. Results for all configurations are presented in appendix in Tab. 5 to Tab. 12. To facilitate the analyze of the results, the range of error ($\delta = max - min$) for each configurations / options are regrouped in Tab 13 and 14 (also presented in appendix). In this section, only the most pertinent results are presented to illustrate the differences between various options and methodologies

4.3.1 Mesh splitting and tracking polynomial order

The first parameter to look at is the convergence of the calculations regarding the mesh splitting and the tracking polynomial order. Tab. 2 presents the results using cross-sections corrected with the classical Selengut for two configurations : #5 and #6. Results shows that most of the gain can be obtained either by increasing the mesh splitting from 4x4* to 8x8* or increasing the polynomial order (DUAL 2 3 to DUAL 3 3). However, not much additional gain is obtained using fine mesh and high polynomial order for the tracking.

The results with coarse mesh and high polynomial order are used in the remaining part of the report to analyze the different options.

TABLE 2 – Relative error between reconstruction and transport calculations (%), mesh and tracking order influence, SELE_FD option in SPH : module

		Heterogeneous (het2)			
		min	max	rms	δ
		4x4*			
C5	DUAL 2 3	-2.45	3.75	0.94	6.19
	DUAL 3 3	-2.24	3.70	0.90	5.94
		8x8*			
C5	DUAL 2 3	-2.53	3.56	0.91	6.09
	DUAL 3 3	-2.40	3.47	0.90	5.86
		min	max	rms	δ
		4x4*			
C6	DUAL 2 3	-6.42	2.64	1.80	9.06
	DUAL 3 3	-6.12	1.77	1.72	7.89
		8x8*			
C6	DUAL 2 3	-6.48	2.00	1.69	8.48
	DUAL 3 3	-5.89	1.93	1.68	7.83

4.3.2 Homogenization geometry

Three geometries for homogenization have been tested. Their results were compared to the performance obtained with a pin-by-pin geometry. Results are presented in Tab. 3 . They were obtained with cross-section normalized with the classical Selengut method. The best option is the heterogeneous geometry 'het2' were the two outer rows of pins are used in the heterogeneous homogenization. In general the root mean square of the error is the minimum for this option.

TABLE 3 – Relative error between reconstruction and transport calculations (%), coarse mesh, SELE_FD option in SPH : module

		Pin by Pin				Heterogeneous (het2) 4x4*				Heterogeneous (het1) 4x4*				Homogeneous 4x4			
		min	max	rms	δ	min	max	rms	δ	min	max	rms	δ	min	max	rms	δ
C1	DUAL 2 3	-6.15	4.99	1.51	11.14	-2.46	3.93	1.35	6.39	-5.48	5.70	1.92	11.17	-7.70	7.15	1.83	14.85
	DUAL 3 3	-	-	-	-	-2.55	3.49	1.31	6.04	-4.88	5.97	1.63	10.85	-2.97	6.62	1.33	9.60
C2	DUAL 2 3	-5.76	4.61	1.67	10.37	-2.54	3.42	1.53	5.96	-4.52	5.13	1.94	9.65	-6.46	6.03	1.81	12.49
	DUAL 3 3	-	-	-	-	-2.42	3.31	1.50	5.73	-4.46	5.50	1.75	9.95	-2.70	5.93	1.50	8.63
C3	DUAL 2 3	-4.40	5.48	1.63	9.88	-3.01	2.51	1.27	5.52	-4.94	5.22	1.97	10.16	-4.89	5.11	1.75	10.00
	DUAL 3 3	-	-	-	-	-3.04	2.52	1.21	5.56	-5.13	4.34	1.65	9.47	-3.03	2.70	1.11	5.72
C4	DUAL 2 3	-1.88	1.75	1.08	3.63	-1.58	2.01	1.01	3.59	-2.17	2.46	1.16	4.63	-1.52	1.84	1.09	3.36
	DUAL 3 3	-	-	-	-	-1.50	1.62	0.99	3.13	-2.11	1.99	1.11	4.10	-1.43	1.86	1.09	3.29
C5	DUAL 2 3	-5.59	5.26	1.25	10.85	-2.45	3.75	0.94	6.19	-4.89	6.06	1.47	10.95	-6.12	5.39	1.31	11.50
	DUAL 3 3	-	-	-	-	-2.24	3.70	0.90	5.94	-4.25	6.16	1.26	10.41	-2.53	5.60	0.89	8.13
C6	DUAL 2 3	-7.37	4.99	1.73	12.36	-6.42	2.64	1.80	9.06	-9.04	6.29	2.33	15.33	-8.86	3.71	2.09	12.58
	DUAL 3 3	-	-	-	-	-6.12	1.77	1.72	7.89	-8.57	2.66	1.87	11.23	-6.09	2.11	1.58	8.20
C7	DUAL 2 3	-5.76	8.31	2.41	14.06	-4.13	4.75	1.69	8.88	-6.37	8.20	2.49	14.57	-5.90	7.42	2.15	13.32
	DUAL 3 3	-	-	-	-	-4.39	4.66	1.61	9.05	-6.80	7.35	2.29	14.15	-4.17	5.13	1.62	9.30
C8	DUAL 2 3	-4.25	3.21	1.90	7.46	-3.09	4.16	1.77	7.25	-5.02	5.67	2.60	10.69	-5.62	4.84	2.37	10.47
	DUAL 3 3	-	-	-	-	-3.05	3.68	1.69	6.73	-4.63	5.13	2.07	9.77	-2.99	3.64	1.68	6.63
C9	DUAL 2 3	-0.14	0.15	0.05	0.29	-0.10	0.11	0.04	0.22	-0.10	0.12	0.04	0.22	-0.10	0.12	0.04	0.22
	DUAL 3 3	-	-	-	-	-0.10	0.11	0.04	0.22	-0.10	0.11	0.04	0.22	-0.10	0.12	0.04	0.22
C10	DUAL 2 3	-1.84	1.31	0.88	3.15	-2.95	1.80	0.97	4.74	-3.45	2.26	1.03	5.71	-2.41	1.84	0.93	4.25
	DUAL 3 3	-	-	-	-	-2.12	1.49	0.95	3.61	-2.24	1.61	0.94	3.85	-1.98	1.54	0.91	3.51
C11	DUAL 2 3	-5.26	4.20	1.77	9.47	-2.76	4.57	1.76	7.33	-4.79	6.03	2.19	10.82	-6.93	7.26	2.09	14.19
	DUAL 3 3	-	-	-	-	-2.50	4.10	1.73	6.60	-3.96	5.73	1.91	9.69	-2.29	5.51	1.70	7.80
C12	DUAL 2 3	-0.34	0.35	0.13	0.69	-0.34	0.33	0.12	0.67	-0.37	0.34	0.13	0.71	-0.34	0.33	0.12	0.67
	DUAL 3 3	-	-	-	-	-0.34	0.33	0.12	0.68	-0.33	0.33	0.12	0.67	-0.34	0.33	0.12	0.67

In addition to the four types of diffusion calculations (4x4, 8x8, 4x4* and 8x8*), the flux has also been computed in diffusion for a pin by pin geometry. For an easier comparison of the error distribution between the different option that may be chosen in the diffusion calculations, three maps of numerical values are presented on Fig. 4 to 6. They represent the difference between the transport and diffusion pin power calculations for pin by pin, heterogeneous (4x4* - 'het2') and homogeneous(4x4) homogenized assemblies respectively for configuration #5. The cross-section normalized with the classical Selengut method (SELE_FD) were used to performed the diffusion calculations with the Raviart-Thomas solver (DUAL 3 3 in `TRIVAT:` module). As previously mentioned, the best results are obtained with the heterogeneous geometry. Results are even generally better than with the pin-by-pin geometry. These results are similar to those obtained by Fliscounakis et al [1].

FIGURE 4 – Relative error between reconstruction and transport calculations for case 5(%), Pin-by-pin

-0.5	-0.5	-0.5	-0.6	-0.6	-0.5	-0.5	-0.9	-0.9	-0.9	-0.9	-0.5	-0.5	-0.6	-0.6	-0.6	-0.6	-0.6	-0.6	-0.7	-0.6	-0.7	-0.6	-0.6	-1.0	-0.9
-0.6	-0.1	-0.1	-0.5	-0.1	-0.2	-0.2	-0.5	-0.9	-0.9	-0.5	-0.3	-0.3	-0.2	-0.6	-0.2	-0.2	-0.7	-0.1	-0.2	-0.6	-0.2	-0.3	-0.3	-0.6	-1.0
	-0.1	-0.3		-0.2	-0.2	-0.2	-0.2	-0.5	-0.6	-0.2	-0.2	-0.2	-0.3		-0.3	-0.2		-0.2	-0.4		-0.3	-0.3	-0.3	-0.3	-0.6
-0.2	-0.2	-0.1	-0.2	-0.2		-0.2	-0.2	-0.5	-0.5	-0.2	-0.2		-0.2	-0.2	-0.2	-0.3	-0.3	-0.3	-0.2	-0.3	-0.3		-0.3	-0.3	-0.6
-0.1	-0.2	-0.2	-0.2	-0.1	-0.2	-0.2	-0.1	-0.6	-0.6	-0.2	-0.2	-0.2	-0.1	-0.3	-0.2	-0.2	-0.2	-0.2	-0.2	-0.3	-0.1	-0.3	-0.3	-0.2	-0.7
	-0.2	-0.2		-0.2	-0.2		-0.6	-0.5	-0.5	-0.6		-0.2	-0.3		-0.2	-0.2		-0.3	-0.2		-0.3	-0.3		-0.6	-0.6
-0.3	-0.1	-0.2	-0.2	-0.1	-0.1	-0.3	-0.1	-0.5	-0.6	-0.1	-0.3	-0.1	-0.2	-0.2	-0.3	-0.2	-0.3	-0.2	-0.2	-0.2	-0.2	-0.2	-0.4	-0.2	-0.7
-0.1	-0.1	-0.1	-0.1	-0.1	-0.2	-0.1	-0.1	-0.5	-0.5	-0.1	-0.1	-0.2	-0.2	-0.2	-0.2	-0.3	-0.2	-0.3	-0.2	-0.3	-0.2	-0.3	-0.2	-0.1	-0.6
	-0.1	-0.2		-0.0	-0.2		-0.6	-0.5	-0.5	-0.6		-0.2	-0.1		-0.3	-0.2		-0.2	-0.3		-0.2	-0.3		-0.7	-0.6
-0.1	-0.1	0.0	-0.1	-0.1	-0.1	-0.0	-0.0	-0.5	-0.5	-0.1	-0.1	-0.2	-0.2	-0.2	-0.1	-0.3	-0.2	-0.3	-0.2	-0.2	-0.2	-0.3	-0.2	-0.2	-0.6
0.0	0.1	0.0	0.0	0.0	0.1	-0.1	0.1	-0.4	-0.5	-0.0	-0.2	-0.1	-0.1	-0.2	-0.1	-0.3	-0.2	-0.3	-0.2	-0.2	-0.2	-0.3	-0.2	-0.2	-0.6
	0.1	0.2		0.1	0.1		-0.3	-0.3	-0.4	-0.5		-0.2	-0.2		-0.2	-0.2		-0.2	-0.2		-0.3	-0.2		-0.6	-0.6
0.5	0.4	0.5	0.3	0.5	0.4	0.2	0.3	-0.3	-0.3	0.0	-0.1	-0.1	0.0	-0.2	-0.1	-0.2	-0.1	-0.2	-0.2	-0.3	-0.1	-0.2	-0.3	-0.2	-0.6
1.0	0.9	1.0	0.9	0.8		0.6	0.5	0.1	-0.1	0.1	-0.0		-0.1	-0.2	-0.1	-0.2	-0.2	-0.2	-0.1	-0.2	-0.2		-0.2	-0.3	-0.5
	1.7	1.6		1.5	1.3	1.2	1.0	0.4	0.1	0.2	0.1	-0.0	-0.1		-0.2	-0.1		-0.1	-0.3		-0.2	-0.2	-0.2	-0.3	-0.5
2.5	3.1	3.1	2.4	2.9	2.7	2.4	1.7	0.8	0.3	0.3	0.2	0.1	0.0	-0.5	-0.0	-0.1	-0.6	-0.1	-0.1	-0.6	-0.2	-0.2	-0.2	-0.5	-0.9
5.2	5.3	5.2	5.2	5.1	4.9	4.4	3.2	2.3	1.0	0.3	0.1	-0.1	-0.3	-0.4	-0.5	-0.5	-0.5	-0.5	-0.6	-0.5	-0.6	-0.5	-0.6	-0.9	-0.9
-3.8	-3.7	-3.7	-3.7	-3.8	-3.9	-4.0	-4.5	-5.6	2.2	0.8	0.4	0.1	-0.3	-0.3	-0.4	-0.5	-0.5	-0.5	-0.5	-0.5	-0.6	-0.5	-0.5	-0.9	-0.9
-0.5	-0.1	-0.3	-0.4	-0.3	-0.7	-1.2	-2.4	-4.5	3.2	1.7	1.0	0.5	0.3	-0.3	0.1	-0.0	-0.6	-0.1	-0.1	-0.6	-0.1	-0.2	-0.2	-0.5	-0.9
	1.1	0.8		1.0	0.9	0.5	-1.2	-4.0	4.4	2.4	1.2	0.6	0.2		-0.1	-0.0		-0.1	-0.3		-0.2	-0.2	-0.2	-0.2	-0.5
1.3	1.5	1.8	1.4	1.4		0.9	-0.7	-3.9	4.9	2.7	1.3		0.4	0.1	0.1	-0.1	-0.2	-0.2	-0.1	-0.2	-0.2		-0.2	-0.2	-0.5
2.2	1.9	1.9	1.7	1.8	1.4	1.0	-0.3	-3.8	5.1	2.9	1.5	0.8	0.5	0.1	0.0	-0.1	-0.0	-0.1	-0.1	-0.2	-0.1	-0.2	-0.2	-0.1	-0.6
	1.9	1.9		1.7	1.4		-0.4	-3.7	5.2	2.4		0.9	0.3		0.0	-0.1		-0.1	-0.2		-0.2	-0.2		-0.5	-0.6
1.9	2.1	2.0	1.9	1.9	1.8	0.8	-0.3	-3.7	5.2	3.1	1.6	1.0	0.5	0.2	0.0	0.0	-0.2	-0.1	-0.2	-0.2	-0.2	-0.1	-0.3	-0.1	-0.5
2.1	2.0	2.1	1.9	1.9	1.5	1.1	-0.1	-3.7	5.3	3.1	1.7	0.9	0.4	0.1	0.1	-0.1	-0.1	-0.1	-0.1	-0.2	-0.2	-0.2	-0.1	-0.1	-0.5
	2.1	1.9		2.2	1.3		-0.5	-3.8	5.2	2.5		1.0	0.5		0.0	-0.1		-0.1	-0.3		-0.1	-0.2		-0.6	-0.5

FIGURE 5 – Relative error between reconstruction and transport calculations for case 5(%), het2 - split 4x4* - DUAL 3 3

-0.6	-0.6	-0.5	-0.6	-0.6	-0.6	-0.5	-0.9	-0.9	-0.9	-0.9	-0.6	-0.6	-0.6	-0.6	-0.6	-0.6	-0.6	-0.6	-0.7	-0.6	-0.7	-0.6	-0.6	-1.0	-1.0
-0.6	-0.1	-0.2	-0.5	-0.2	-0.2	-0.3	-0.5	-1.0	-0.9	-0.5	-0.3	-0.3	-0.2	-0.6	-0.2	-0.2	-0.7	-0.1	-0.3	-0.6	-0.3	-0.3	-0.4	-0.6	-1.0
	-0.1	-0.3		-0.2	-0.2	-0.2	-0.3	-0.6	-0.6	-0.3	-0.2	-0.2	-0.3		-0.3	-0.2		-0.2	-0.4		-0.3	-0.3	-0.3	-0.4	-0.6
-0.2	-0.2	-0.1	-0.2	-0.2		-0.2	-0.2	-0.5	-0.6	-0.2	-0.2		-0.2	-0.2	-0.2	-0.3	-0.3	-0.3	-0.2	-0.3	-0.3		-0.3	-0.3	-0.6
-0.1	-0.2	-0.2	-0.2	-0.1	-0.2	-0.2	-0.2	-0.6	-0.6	-0.2	-0.2	-0.3	-0.1	-0.3	-0.3	-0.3	-0.2	-0.3	-0.3	-0.3	-0.1	-0.3	-0.3	-0.3	-0.7
	-0.2	-0.2		-0.2	-0.2		-0.5	-0.5	-0.6	-0.5		-0.2	-0.3		-0.3	-0.2		-0.2	-0.2		-0.3	-0.3		-0.6	-0.6
-0.2	-0.1	-0.2	-0.2	-0.2	-0.1	-0.2	-0.2	-0.5	-0.6	-0.2	-0.3	-0.2	-0.2	-0.2	-0.3	-0.2	-0.3	-0.2	-0.3	-0.2	-0.3	-0.2	-0.4	-0.3	-0.7
-0.1	-0.1	-0.1	-0.1	-0.2	-0.2	-0.1	-0.1	-0.5	-0.5	-0.1	-0.2	-0.2	-0.2	-0.2	-0.2	-0.3	-0.2	-0.3	-0.2	-0.2	-0.3	-0.3	-0.2	-0.1	-0.6
	-0.3	-0.3		-0.2	-0.4		-0.7	-0.7	-0.6	-0.6		-0.2	-0.1		-0.2	-0.2		-0.2	-0.3		-0.2	-0.3		-0.7	-0.6
-0.2	-0.2	-0.1	-0.1	-0.2	-0.2	-0.1	-0.1	-0.5	-0.5	-0.1	-0.1	-0.2	-0.2	-0.2	-0.2	-0.3	-0.2	-0.3	-0.2	-0.2	-0.3	-0.3	-0.2	-0.2	-0.6
0.1	0.2	0.1	0.1	0.1	0.1	-0.0	0.1	-0.4	-0.4	-0.1	-0.2	-0.2	-0.2	-0.2	-0.3	-0.2	-0.2	-0.2	-0.3	-0.3	-0.3	-0.2	-0.3	-0.2	-0.6
	0.2	0.2		0.1	0.2		-0.3	-0.3	-0.4	-0.5		-0.1	-0.2		-0.2	-0.2		-0.2	-0.2		-0.3	-0.2		-0.6	-0.6
0.4	0.3	0.3	0.2	0.3	0.2	0.1	0.1	-0.4	-0.4	-0.1	-0.1	-0.1	-0.0	-0.2	-0.2	-0.2	-0.1	-0.2	-0.2	-0.3	-0.1	-0.2	-0.3	-0.2	-0.6
0.7	0.6	0.6	0.5	0.4		0.3	0.2	-0.2	-0.3	-0.0	-0.1		-0.1	-0.1	-0.2	-0.2	-0.2	-0.2	-0.2	-0.2	-0.3		-0.2	-0.3	-0.6
	1.5	1.3		1.2	1.0	0.9	0.7	0.2	-0.0	0.1	-0.0	-0.1	-0.1		-0.2	-0.1		-0.2	-0.3		-0.2	-0.2	-0.2	-0.3	-0.6
1.7	2.3	2.2	1.5	2.0	2.0	1.7	1.1	0.3	-0.1	0.1	0.1	-0.0	-0.1	-0.5	-0.1	-0.1	-0.6	-0.1	-0.2	-0.5	-0.2	-0.2	-0.3	-0.5	-0.9
3.7	3.4	3.2	3.1	3.3	3.4	2.7	1.7	1.0	0.2	-0.1	-0.0	-0.3	-0.4	-0.4	-0.4	-0.5	-0.6	-0.5	-0.6	-0.6	-0.6	-0.6	-0.6	-0.9	-0.9
-1.9	-1.9	-1.7	-1.5	-1.9	-2.2	-2.1	-2.2	-2.0	1.0	0.3	0.2	-0.2	-0.4	-0.3	-0.4	-0.5	-0.7	-0.5	-0.5	-0.5	-0.6	-0.5	-0.6	-1.0	-0.9
0.7	0.7	0.3	0.5	0.5	0.2	-0.4	-1.1	-2.2	1.7	1.1	0.7	0.2	0.1	-0.3	0.1	-0.1	-0.7	-0.1	-0.2	-0.5	-0.2	-0.2	-0.3	-0.5	-0.9
	1.4	0.9		1.5	1.8	1.0	-0.4	-2.1	2.7	1.7	0.9	0.3	0.1		-0.0	-0.1		-0.1	-0.2		-0.2	-0.2	-0.2	-0.3	-0.5
2.1	2.0	2.0	1.7	2.0		1.8	0.2	-2.2	3.4	2.0	1.0		0.2	0.2	0.1	-0.2	-0.4	-0.2	-0.1	-0.2	-0.2		-0.2	-0.2	-0.6
2.9	2.2	2.0	1.8	2.1	2.0	1.5	0.5	-1.9	3.3	2.0	1.2	0.4	0.3	0.1	0.1	-0.2	-0.2	-0.2	-0.2	-0.2	-0.1	-0.2	-0.2	-0.2	-0.6
	2.1	1.9		1.8	1.7		0.5	-1.5	3.1	1.5		0.5	0.2		0.1	-0.1		-0.1	-0.2		-0.2	-0.2		-0.5	-0.6
2.4	2.2	1.9	1.9	2.0	2.0	0.9	0.3	-1.7	3.2	2.2	1.3	0.6	0.3	0.2	0.1	-0.1	-0.3	-0.1	-0.2	-0.2	-0.2	-0.1	-0.3	-0.2	-0.5
2.8	2.4	2.2	2.1	2.2	2.0	1.4	0.7	-1.9	3.4	2.3	1.5	0.6	0.3	0.2	0.2	-0.2	-0.3	-0.1	-0.1	-0.2	-0.2	-0.2	-0.1	-0.1	-0.6
	2.8	2.4		2.9	2.1		0.7	-1.9	3.7	1.7		0.7	0.4		0.1	-0.2		-0.1	-0.2		-0.1	-0.2		-0.6	-0.6

FIGURE 6 – Relative error between reconstruction and transport calculations for case 5(%), het0 - split 4x4* - DUAL 3 3

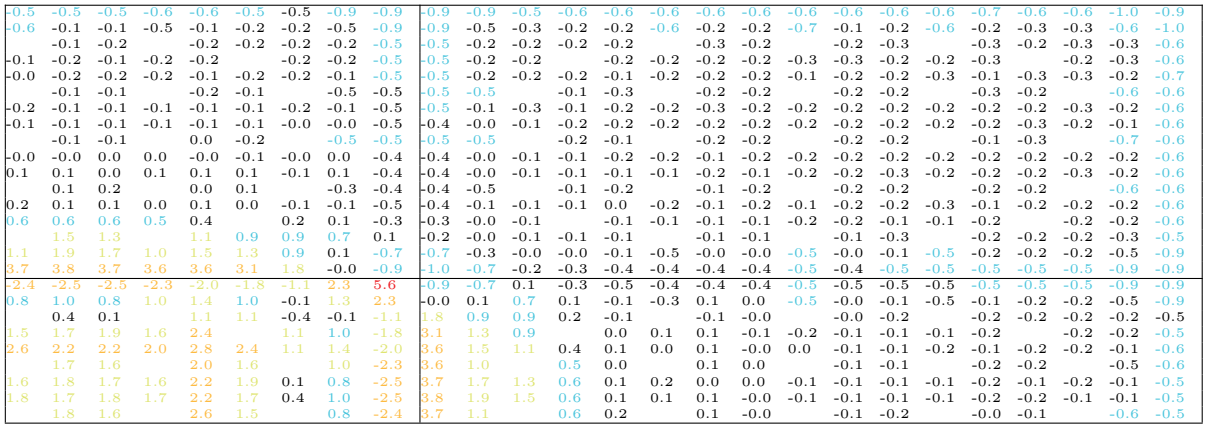

4.3.3 Homogenization SPH option

The last option to compare is the choice of SPH method. The results for flux-volume (STD), classical Selengut (SELE_FD) and Selengut macro-calculation water gap (SELE_MWG) are presented in Tab. 4. This table shows that the flux-volume homogenization leads to fairly large errors. The smallest range of errors are generally obtained with the classical Selengut option. Regarding the error distribution, the results for the root mean square obtained with the Selengut macro-calculation water gap are comparable to those obtained with the classical Selengut, sometime better sometime worst depending on the configuration.

TABLE 4 – Relative error between reconstruction and transport calculations (%), coarse mesh,

		'SELE_FD' 4x4*				'SELE_MWG' 4x4*				'STD' 4x4*			
		min	max	rms	δ	min	max	rms	δ	min	max	rms	δ
C1	DUAL 2 3	-2.46	3.93	1.35	6.39	-3.64	6.75	1.68	10.39	-5.39	13.69	2.27	19.08
	DUAL 3 3	-2.55	3.49	1.31	6.04	-2.02	6.32	1.38	8.34	-4.88	17.76	1.90	22.64
C2	DUAL 2 3	-2.54	3.42	1.53	5.96	-2.76	6.21	1.67	8.97	-4.33	11.82	2.18	16.15
	DUAL 3 3	-2.42	3.31	1.50	5.73	-2.21	6.13	1.47	8.34	-4.50	15.92	1.95	20.41
C3	DUAL 2 3	-3.01	2.51	1.27	5.52	-2.92	3.66	1.83	6.58	-6.34	5.70	2.07	12.04
	DUAL 3 3	-3.04	2.52	1.21	5.56	-3.08	3.51	1.57	6.58	-8.75	7.63	1.57	16.38
C4	DUAL 2 3	-1.58	2.01	1.01	3.59	-1.44	2.19	0.90	3.63	-2.60	3.60	1.20	6.20
	DUAL 3 3	-1.50	1.62	0.99	3.13	-1.27	1.44	0.83	2.71	-2.78	3.92	1.18	6.70
C5	DUAL 2 3	-2.45	3.75	0.94	6.19	-2.91	5.59	1.32	8.49	-3.89	11.16	1.62	15.06
	DUAL 3 3	-2.24	3.70	0.90	5.94	-1.36	5.41	1.16	6.77	-4.29	15.22	1.33	19.51
C6	DUAL 2 3	-6.42	2.64	1.80	9.06	-7.96	4.76	2.31	12.72	-8.97	6.66	2.47	15.62
	DUAL 3 3	-6.12	1.77	1.72	7.89	-6.99	2.90	1.87	9.88	-8.94	3.37	2.05	12.31
C7	DUAL 2 3	-4.13	4.75	1.69	8.88	-3.55	4.91	1.47	8.46	-9.02	7.93	2.24	16.94
	DUAL 3 3	-4.39	4.66	1.61	9.05	-4.03	3.34	1.25	7.37	-11.67	10.84	1.73	22.51
C8	DUAL 2 3	-3.09	4.16	1.77	7.25	-4.22	6.18	2.60	10.40	-6.01	8.50	3.01	14.51
	DUAL 3 3	-3.05	3.68	1.69	6.73	-3.78	5.58	2.15	9.36	-6.85	8.83	2.54	15.69
C9	DUAL 2 3	-0.10	0.11	0.04	0.22	-0.13	0.14	0.05	0.27	-0.10	0.12	0.04	0.22
	DUAL 3 3	-0.10	0.11	0.04	0.22	-0.13	0.14	0.05	0.27	-0.10	0.12	0.04	0.22
C10	DUAL 2 3	-2.95	1.80	0.97	4.74	-2.72	2.27	0.78	4.99	-2.46	1.77	0.98	4.23
	DUAL 3 3	-2.12	1.49	0.95	3.61	-1.56	1.09	0.59	2.65	-2.13	1.63	0.96	3.75
C11	DUAL 2 3	-2.76	4.57	1.76	7.33	-3.19	7.29	1.90	10.48	-4.49	12.95	2.49	17.44
	DUAL 3 3	-2.50	4.10	1.73	6.60	-2.05	6.79	1.57	8.84	-4.18	15.05	2.18	19.24
C12	DUAL 2 3	-0.34	0.33	0.12	0.67	-0.49	0.35	0.15	0.84	-0.34	0.33	0.12	0.67
	DUAL 3 3	-0.34	0.33	0.12	0.68	-0.42	0.34	0.15	0.77	-0.34	0.33	0.12	0.67

To better understand the performance of those two Selengut options, maps of the error have been plot on Fig. 7. The graphs show that the flux is more continuous at the assembly interfaces with the Selengut macro-calculation water gap. This result shows that this new Selengut method has been correctly implemented and that it guaranties the flux continuity at the assembly interface as designed to.

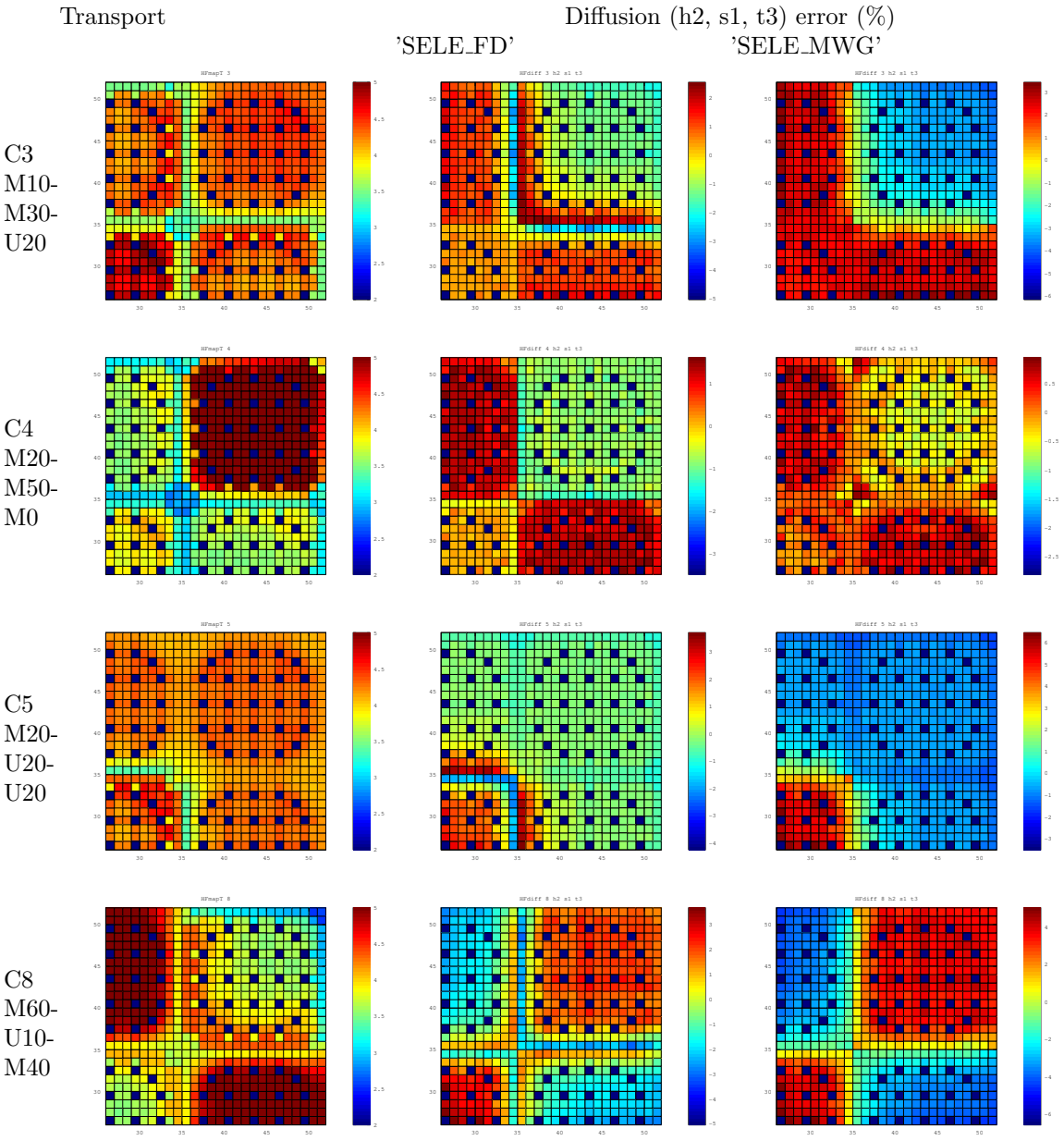

FIGURE 7 – Transport vs diffusion pin power distribution, comparison 'SELE_FD' and 'SELE_MWG' SPH options

5 Modules and data structures

5.1 DONJON

The implementation of pin-power reconstruction in DRAGON / DONJON has required several changes in the code. A new module named `NAP:` has been programmed to perform the PPR.

As seen in the previous sections, heterogeneous assemblies are simulated. In order to be able to handle these configurations, several modifications had to be done to the existing modules. These modifications serve two main purposes :

- Automatic geometry definition.
- Pre-format results for pin-power reconstruction.

On a practical point of view, several modules had to be changed and their user guide updated :

- `RESINI:` This module of DONJON is used to initialize the MAP data structure (`L_MAP` signature). This structure contains the description of the fuel channels. In PWR cases, each channel corresponds to an assembly. Using heterogeneous mixtures in one assembly increases the complexity of the geometry. However, two levels geometries (embedded geometry) are not possible in the DONJON code. The general idea is then to define one channel per mixture for all assemblies. All these channels have then to be regrouped by assembly to impose the same burnup. This process could be done manually, but if the heterogeneity of the cross-section is large (ex. one mixture per pin within a complete core), the geometry definition may be too complex. This task can be performed automatically by the module `NAP:`.
- `NCR:` This component of the lattice code is dedicated to the interpolation of MICROLIB and MACROLIB data from a MULTICOMPO object, the reactor database produced by `COMPO:`. In the context of the pin power reconstruction, this module has to be slightly modified when the geometry and the embedded geometry of the RESINI object have been modified by the `NAP:` module. In that case, new mixture numbers have been automatically assigned to the regions, thus association between mixture numbers and cross-sections in the *COMPO* objects has to be done automatically to guaranty the coherence.
- `USPLIT:` This module is used to create a `MATEX` object that will provide a link between the reactor geometry and material index.

The new options of these modules and the `NAP:` module are described in the DONJON v5 user guide [10]. The additional information also stored in the data-structures is also presented in the user guide.

5.2 DRAGON

A new methodology has been introduced for cross-section homogenization as described in Section 2.2.3 : Selengut water gap normalization. The `SPH:` module has been changed to perform this approach. The description of the news option is presented in the user guide [11].

The geometry data-structure stores additional information regarding the assemblies. The new features are described in [12].

5.3 TRIVAC

A new module named `VAL:` has been developed to interpolate the flux in diffusion calculations for Cartesian geometries. The description of the module is presented in [13]. The data-structure created by the `VAL:` module has 'F_VIEW' as signature. It is described in [12]. An example of the post-processing of the results is presented in the '*my_version5_path*/Octave/data/iaea3d.m' procedure.

5.4 Octave

Octave is a free software equivalent to the commercial software MATLAB. Except for few restrictions, the same input files can be used in both softwares.

A set of procedures (named 'ASCII-Ganlibv4') has been developed to facilitate analysis from DRAGON and DONJON results. They provide tools to access rapidly and efficiently the content of data structures saved in ASCII format. For more details, please refers to the 'readme' file in the folder '*my_version5_path*/Octave/'.

6 Conclusions and recommandations

In this report, we have presented how the generalized pin power reconstruction has been successfully implemented in DRAGON-DONJON v5. A new module called `NAP:` has been programmed to perform the following tasks :

- Enrich MULTICOMPO to store pin-wise projected flux of diffusion calculation of homogenized assembly in an infinite domain. The process can be repeated several times on the same data structure for different homogenization / diffusion calculation options.
- Automatic generation of a two level geometry (core with heterogeneous assemblies) as a one level geometry
- Compute reconstructed pin power.

During the validation of the method, we have emphasized that it is highly recommended to perform an interpolation of the flux within macro regions before projecting it on the pins. This interpolation is done using the polynomial representation used by the flux solver (such as Raviart-Thomas in our case). A lower order of the polynomial (mainly flat flux approximation) can lead to less precise results, especially if the macro-regions are large and there is a great deal of heterogeneity between and inside assemblies.

To validate our implementation of the method, 12 configurations of 3x3 cluster of PWR-900 assemblies have been simulated. They are the same as those used by Fliscounakis in [1] plus two homogeneous clusters. First, the homogeneous cluster results are very good. The difference between transport and diffusion calculations are smaller than 0.15% for UOX and 0.4% for MOX.

With regards to the SPH homogenization, the flux-volume normalization has demonstrated large errors and is not recommended even when using an heterogeneous assembly. All Selengut methods are better than the flux-volume homogenization. When compared together, the classical Selengut method leads to the smallest range of errors in general which is the main criteria to choose between the SPH homogenization methods. On the other hand, the Selengut macro-calculation water gap method presents better results regarding flux continuity at assembly interface. This result was expected since Selengut macro-calculation water gap method is designed to guaranty flux continuity in diffusion, whereas classical Selengut is designed to guaranty the flux in transport.

In conclusion, the Flux-Volume normalization is not recommended because of unprecise results. Althought, the Selengut macro-calculation water gap normalization does not produce the most accurate results, it should not be completely overlooked because of the promising tendencies regarding flux continuity at assembly interfaces. Finally, we recommend the use of the classical Selengut normalization because it minimizes the maximum and the root mean square errors in a broader range of configurations, which makes this method more reliable.

A Detailed algorithm

A.1 Detailed algorithm and input file description

The detailed algorithm refers to the three main steps of the general algorithm presented previously. They can be summarized as follows :

Step #1 DRAGON : compute usual cross-sections for homogeneous, heterogeneous and pin-by-pin assembly
↓
MULTICOMPO
↓
Step #2 DONJON : compute flux on infinite domain for each homogenization type
↓
MULTICOMPO 'enriched' (including $\psi^{d,\infty}_{m,p}$)
↓
Step #3 DONJON : Compute core flux and perform pin-power reconstruction

A.1 Step #1

The general procedure to compute a regular MULTICOMPO for a PWR can be found in the example '*rep900_mco.x2m*' and its procedure folder which are included within the distribution . In this section, we want to concentrate on the specific changes that have been done to include the specificities required by pin-power reconstruction, and leads to the new set of input files : '*rep900het_mco.x2m*'. As previously said, two main additions are done :

1. Pin-power reconstruction requires datas for several types of homogenization as the same time. The first change is then to perform several homogenizations after the flux calculation, and to store the results in the same MULTICOMPO (in different records) to facilitate the data handling in the core computations.
2. Homogenized geometry must be recorded in the MULTICOMPO. **Note : The included geometry in the multicompo has to be unfolded, even if the transport calculations are done on a 1/8th assembly. Moreover no split can be defined in the geometry, one mesh ONLY per heterogeneous mixture is mandatory.**

The detailed algorithm to compute a regular MULTICOMPO with the additions can then be summarized as follows :

0 : Define the MULTICOMPO structure (parameter names and types)
Define geometry and tracking for

level	self-shielding	1	2
tracking module	`SYBILT:`	`SYBILT:`	`NXT:` and `MCCGT:`
#energy groups :	281	281	26

Define homogenized geometries to store in the MULTICOMPO (GEOTMP) :

homogeneous (homog)	heterogeneous #1 (het1)	heterogeneous #2 (het2)	heterogeneous #3 (het3)	Pin-by-pin (pbp)
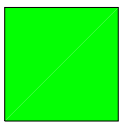	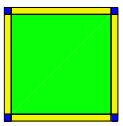	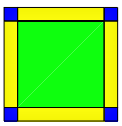	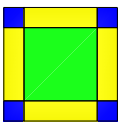	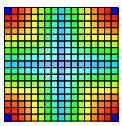

Define homogenization geometries used by the `SPH:` module (ASSMB_HOM) :

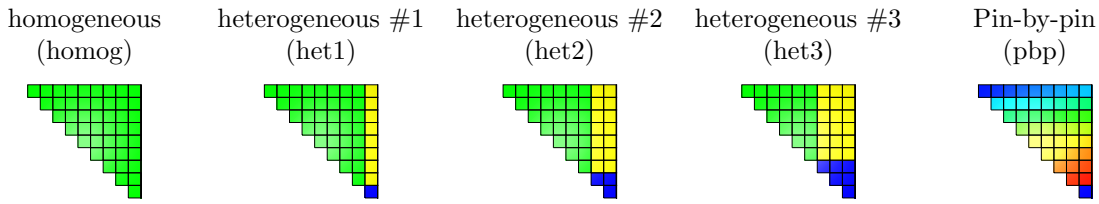

1 : Reference depletion

(a) Set all parameters at reference value

(b) Loop on all burnup steps :

- Compute cross-sections
- Perform self-shielding (if required)
- Perform flux calculations at level 1
- Perform flux calculations at level 2
- Perform homogenization and include homogenized geometry (GEOTMP)

```
EDIOBJ := EDI: FLUX2 LIBEQ TRACKN2 GEON2 GEOTMP ::
MERG REGI
...
MGEO GEOTMP ;
```

- Perform SPH factor calculations using homogenization geometry (ASSMB_HOM)

- *Save data in* MULTICOMPO
  ⇒ isotopic concentration at each burnup step (BURNUP structure)

2 : Perturbation calculations

- For each parameter :

  - loop on each perturbed value (except reference value) :

    - loop on each burnup step :
      Get isotopic concentration from BURNUP structure
      Compute flux distribution
      Perform homogenization with 'ASSMB_HOM' and include homogenized geometry (GEOTMP)
      Save data in MULTICOMPO

A.2 Step #2

This step is closely related to the previous one. Knowing the structure of a regular MULTICOMPO is required to enrich it. Indeed, for each calculation, parameter value have to be recover. It is recommended to start from the input files used to create the original MULTICOMPO to write the input files used to enrich the MULTICOMPO. This way, the same loops for all parameter values will be used and none will be forgotten or added. An example of set of input files is provided in '*rep900EnrichCOMPO.x2m*'. It is related to the set of input files : '*rep900het_mco.x2m*'.

The detailed algorithm to enrich a regular MULTICOMPO with the additional data can then be summarized as follows :

0 : Define the homogenized geometry. It can be recovered from the MULTICOMPO. Do not use symmetry nor split.

For all calculations in MULTICOMPO, perform the following :

1 : Set parameter values

2 : Get cross-sections from homogenized data and create a MACROLIB (`NCR:` + `MACINI:`)

3 : Compute flux (`TRIVAT:` + `FLUD:`)

4 : **Project flux on each pin : compute** $\phi_{i,p}^{\infty}$. This is done with the `NAP:` module with the `PROJECTION` keyword. Here is an example :

```
Cpo := NAP: Cpo Track Flux ::
  EDIT 0
  PROJECTION
    DIRPIN <<DirPin>>
    IFX 2
    SET  'burnup' <<burnup>>
    SET  'ppmBore'   <<ppmBore>>
    SET  'TF'        8.0000E+02
    SET  'TCA'       6.0000E+02
    SET  'DCA'       6.5900E-01
;
```

We would like to remind here that the pin-wise projected flux is normalized using the flux volume technique as described in Section 2.3.

Note : No fuel is defined with `RESINI:` module. All calculations are performed in 2D directly on the geometry.

A.3 Step #3

0 : Define core geometry (Geo1) with :

(a) **Only ONE mesh along X and Y directions for assemblies. Final mesh for the moderator/coolant parts.**

(b) **Final mesh along Z direction.**

1 : Define Geometries

	Geo1 ↓	Geo1 ↓
a) `NAP:` option DIRGEO	+ Heterogeneous. assembly optional split ↓ GeoH	+ Pin-by-pin assembly **no split** ↓ GeoP
b) `USLPIT:`	↓ MatexH	↓ MatexP
c) `TRIVAT:`	↓ Track	

Here follows an example of a call to the `NAP:` module :

```
GeoH := NAP: Geo1 CpoU ::
  EDIT 0
  DIRGEO <<DirHet>>
  MIXASS 3 1 2 3
  SPLITX-ASS 1 2 1
  SPLITY-ASS 1 2 1
;
```

Notes : A MULTICOMPO is required to get the homogenization geometry. More split at the assembly level along X and Y directions can be defined here.

2 : Define fuel object with `RESINI:` and embedded `NAP:` modules

`RESINI:`	↓ FmapH	↓ FmapP

3 : Compute cross-sections

fuel (`NCR:`)	↓ MacroFH	↓ MacroFP
coolant (`NCR:`)	+ Macro	
core (`MACINI:`)	↓ Macro2H	

4 : Compute flux distribution

`TRIVAA:` + `FLUD:`	↓ Flux	

5 : Perform Pin-Power Reconstruction

	FmapH + Track + Flux + MatexH	FmapP + MacroFP
`NAP:`	↓ FmapH	

To perform the pin-power reconstruction, several cross-section / flux are requiered for each pin for they current burnup / boron concentration and other parameter values. The choice has been made to compute these values by the module designed for that (`NCR:`), which means it is done externaly of the `NAP:` module in order to not duplicate fortran code (for better code maintenance). This approach implies that the fuel position has to be specified pin-by-pin at some point, hence why there are two geometries and two map structures defined in this step of the detail algorithm.

A.2 Automatic geometry generation

When heterogeneous assembly are used in the core calculations, the geometry has to match the heterogeneities in order to put the proper mixtures to corresponding regions in the core. The geometry description of the core and the fuel becomes rapidly complex. The number of mixtures can also be very large. To facilitate the process an automatic geometry definition has been introduced. It is programmed in the `NAP:` module with the keyword `GEODIR`. The sets of input file *'testNAPGEO.x2m'* and *'rep900cluster.x2m'* illustrates this function for a core with 4 planes plus coolant and a core with 1 plane no coolant respectively. A graphical representation before and after automatic definition is presented in Fig. 8.

In this module, assemblies are split according to the heterogeneity of the homogenization. Additional split can be introduced as shown in Step #3 - 1c of the detailed algorithm and illustrated below for the *'testNAPGEO.x2m'* exemple :

```
! Build geometry for homogeneous assembly
Geo1 := GEO: :: CAR3D 5 5 4
  EDIT 1
  X- VOID X+ VOID
  Y- VOID Y+ VOID
  Z- VOID Z+ VOID
  MIX
PLANE 1
    0 4 4 4 0
    4 4 4 4 4
    4 4 4 4 4
    4 4 4 4 4
    0 4 4 4 0
PLANE 2
    0 4 4 4 0
    4 3 2 3 4
    4 2 1 2 4
```

testNAPGEO.x2m
Original
CAR3D 5 5 4

Split

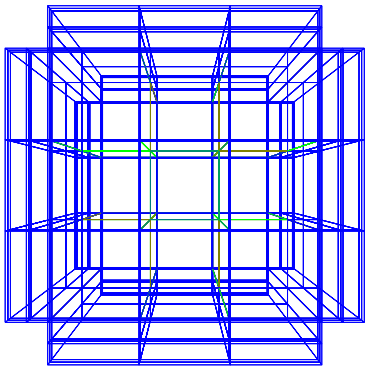

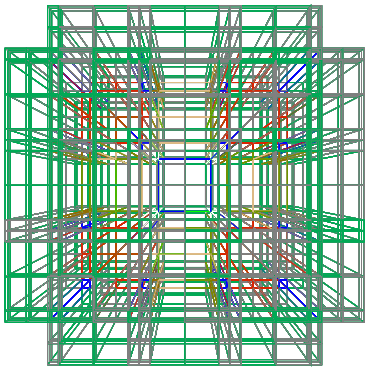

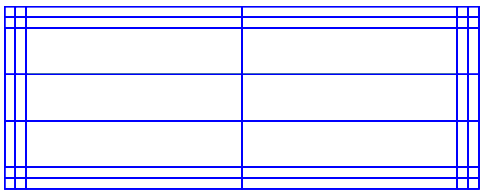

---

rep900cluster.x2m
Original
CAR3D 3 3 1

Split

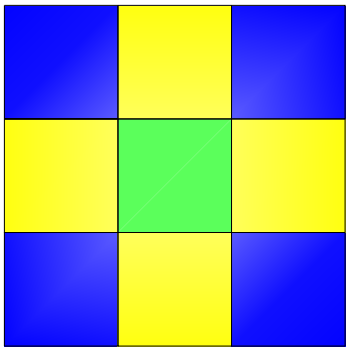

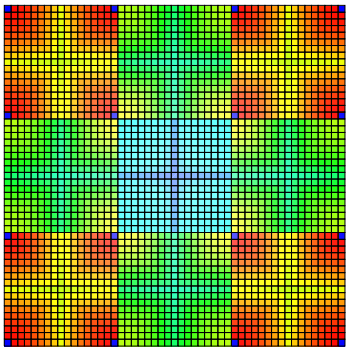

FIGURE 8 – Automatic geometries

```
    4 3 2 3 4
    0 4 4 4 0
PLANE 3 SAME 2
PLANE 4 SAME 1
  MESHX <<mx1>> <<mx2>> <<mx3>> <<mx4>> <<mx5>> <<mx6>>
  MESHY <<mx1>> <<mx2>> <<mx3>> <<mx4>> <<mx5>> <<mx6>>
  MESHZ 0. 10. 110. 210. 220.
  SPLITX 2 1 1 1 2
  SPLITY 2 1 1 1 2
  SPLITZ 2 1 1 2
;
! Build geometry for heterogeneous assembly
GeoH := NAP: Geo1 CpoU ::
  EDIT 10
  DIRGEO <<DirHet>>
  MIXASS 3 1 2 3
  SPLITX-ASS 1 2 1
  SPLITY-ASS 1 2 1
;
```

leads to :

```
 Original mesh corresponding to assemblies
 X direction: AXD(1 : NXD)=   0   1   1   1   0
 Y direction: AYD(1 : NYD)=   0   1   1   1   0
 Splitting within assemblies:
 SXP   1   2   1
 SYP   1   2   1
 New mixtures:
 plane #   1
   0   4   4   4   4   4   4   4   4   4   0
   4   4   4   4   4   4   4   4   4   4   4
   4   4   4   4   4   4   4   4   4   4   4
   4   4   4   4   4   4   4   4   4   4   4
   4   4   4   4   4   4   4   4   4   4   4
   4   4   4   4   4   4   4   4   4   4   4
   4   4   4   4   4   4   4   4   4   4   4
   4   4   4   4   4   4   4   4   4   4   4
   4   4   4   4   4   4   4   4   4   4   4
   4   4   4   4   4   4   4   4   4   4   4
   0   4   4   4   4   4   4   4   4   4   0
 plane #   2
   0   4   4   4   4   4   4   4   4   4   0
   4  13  12  13  10   9  10  13  12  13   4
   4  12  11  12   9   8   9  12  11  12   4
   4  13  12  13  10   9  10  13  12  13   4
   4  10   9  10   7   6   7  10   9  10   4
   4   9   8   9   6   5   6   9   8   9   4
   4  10   9  10   7   6   7  10   9  10   4
   4  13  12  13  10   9  10  13  12  13   4
   4  12  11  12   9   8   9  12  11  12   4
   4  13  12  13  10   9  10  13  12  13   4
   0   4   4   4   4   4   4   4   4   4   0
 plane #   3
   0   4   4   4   4   4   4   4   4   4   0
   4  13  12  13  10   9  10  13  12  13   4
   4  12  11  12   9   8   9  12  11  12   4
```

```
  4  13  12  13  10   9  10  13  12  13   4
  4  10   9  10   7   6   7  10   9  10   4
  4   9   8   9   6   5   6   9   8   9   4
  4  10   9  10   7   6   7  10   9  10   4
  4  13  12  13  10   9  10  13  12  13   4
  4  12  11  12   9   8   9  12  11  12   4
  4  13  12  13  10   9  10  13  12  13   4
  0   4   4   4   4   4   4   4   4   4   0
plane #   4
  0   4   4   4   4   4   4   4   4   4   0
  4   4   4   4   4   4   4   4   4   4   4
  4   4   4   4   4   4   4   4   4   4   4
  4   4   4   4   4   4   4   4   4   4   4
  4   4   4   4   4   4   4   4   4   4   4
  4   4   4   4   4   4   4   4   4   4   4
  4   4   4   4   4   4   4   4   4   4   4
  4   4   4   4   4   4   4   4   4   4   4
  4   4   4   4   4   4   4   4   4   4   4
  4   4   4   4   4   4   4   4   4   4   4
  0   4   4   4   4   4   4   4   4   4   0

Assembly zones:
  1   1   1   2   2   2   3   3   3
  1   1   1   2   2   2   3   3   3
  1   1   1   2   2   2   3   3   3
  4   4   4   5   5   5   6   6   6
  4   4   4   5   5   5   6   6   6
  4   4   4   5   5   5   6   6   6
  7   7   7   8   8   8   9   9   9
  7   7   7   8   8   8   9   9   9
  7   7   7   8   8   8   9   9   9
```

When the geometry is automatically split at assembly level, the fuel mixtures are redefined automatically (as shown in example over). In order to keep all the input files coherent, several parts have to take into account these new mixture numbers. The affected modules are :

1. `USPLIT:` where the fuel mixture numbers are defined and stored.
2. `RESINI:` where the fuel positions are defined and stored.
3. `NCR:` where the fuel cross-sections are computed and stored.

In all these modules, keywords have been added to perform their task for all the new fuel mixtures automatically. The detailed modifications and user guide are presented in [10].

A.3 Verifications

The input files '*rep900het_mco.x2m*', '*rep900EnrichCOMPO.x2m*' and '*rep900cluster.x2m*' have been used to verify the new GPPR capabilities. Results obtained with '*rep900cluster.x2m*', i.e. for the reconstructed pin-power, are compared to a reference transport calculation programmed in the data set : '*rep900cluster_mco.x2m*'. Both transport and diffusion input sets represent a 3x3 cluster with 17x17 pins assemblies. Several clusters have been simulated, all results and important details are presented in Section 4. In this section, only one configuration is used to illustrate the implementation : Case #5. This case corresponds to a cluster 3x3 with the following components :

- a MOX assembly at burnup 20 GWd/t in the center
- 4 UOX assemblies at burnup 20 GWd/t on the sides
- 4 UOX assemblies at burnup 20 GWd/t on the corners

A.1 Verification part 1

The first part to verify is the enrich MULTICOMPO step. Results were directly looked at in enrich MULTICOMPO and two major points were found :

- new properties are added with the proper names at the right place :
  The following code has been repeated 4 times with $<< ifx >>$ equal 0 to 3 :

```
Cpo := NAP: Cpo Track Flux ::
  EDIT 0
  PROJECTION
    DIRPIN <<DirPin>>
    IFX <<ifx>>
    SET  'burnup' <<burnup>>
    SET  'ppmBore'   <<ppmBore>>
```

  This resulted in the following records in the enrich MULTICOMPO :

```
...
->       6      12       3      32                                  <-
ADDXSNAME-P0
         4         4         4         4         4         4         4         4
         4         4         4         4         4         4         4         4
         4         4         4         4         4         4         4         4
         4         4         4         4         4         4         4         4
NFTOT   NG      N2N     N3N     N4N     NA      NP      N2A     NNP     ND
NT      TRANC   FINF_000FINF_001FINF_002FINF_003
...
->       7      12       2       2                                   <-
FINF_000
  4.48785095E+01  4.85739851E+00
->       7      12       2       2                                   <-
FINF_001
  4.51128273E+01  4.73293400E+00
->       7      12       2       2                                   <-
FINF_002
  4.55112991E+01  4.36975765E+00
->       7      12       2       2                                   <-
FINF_003
  4.52058678E+01  4.63550901E+00
...
```

- infinite diffusion projected flux are coherent with original diffusion calculation, and normalization is properly done.

Note that using an edition level at 100 provides a large number of data with several intermediate results in the output in order to verify the calculations.

A.2 Verification part 2

The second part consists of verifying the automatic geometry spliting. This part can be verified again with an edition level equal to 100. It can also be visually verified with the illustrated examples provided in the detailed algorithm description and also in Section A.2.

A.3 Verification part 3

Finally, the last part of the verification is the pin power reconstruction. Two substeps are looked at : the flux projection and then the pin power calculation. The transport geometry of the cluster is presented

on Fig. 9.

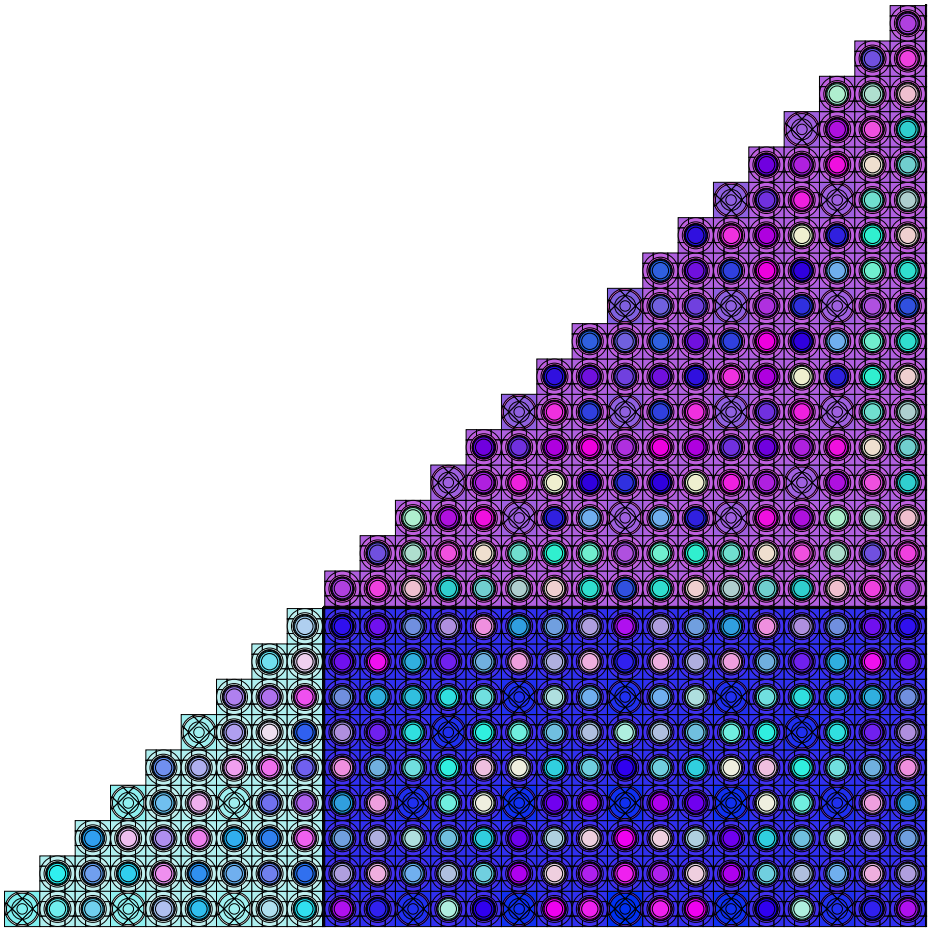

FIGURE 9 – Transport geometry of the cluster

The pin flux (homogenized with surrounding water) computed by transport calculations is presented on top of Fig. 10. The corresponding flux computed by diffusion calculation is also presented on the four remaining graphs. Each graph corresponds to a different configuration : homogeneous or heterogeneous mixtures, split with 4 or 8 meshes along each direction. The left part of the graphs shows the flux distribution on the original core geometry and the right part is the projected flux on each pin (homogenized with surrounding water). Only the top right part of the cluster is presented since the geometry is symmetrical. Note that a very important concerning the flux projection on each pin from macro regions is presented in Section 4.

The reconstructed pin-power is presented on Fig. 11. These pin power distributions correspond to the flux distributions presented on Fig. 10. The difference with reference transport computations are presented on Fig. 12. Results from Fig. 10 to 12 show that the GPPR has been correctly implemented. Flux are properly projected, and pin power relatively agree between transport and diffusion calculations. The different homogenizations and splits lead to more or less precise results according to the choices.

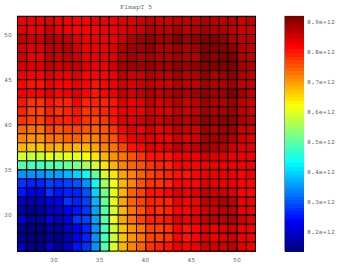

Transport

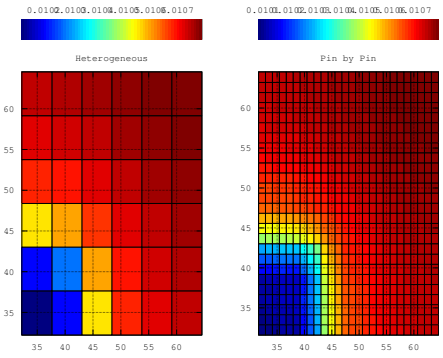

homog. 4x4

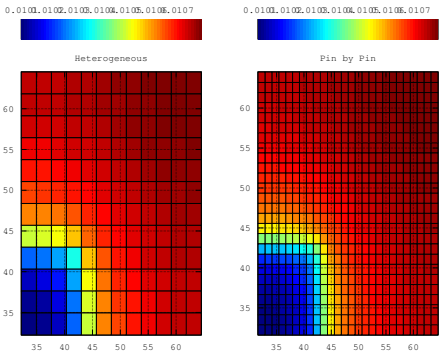

homog. 8x8

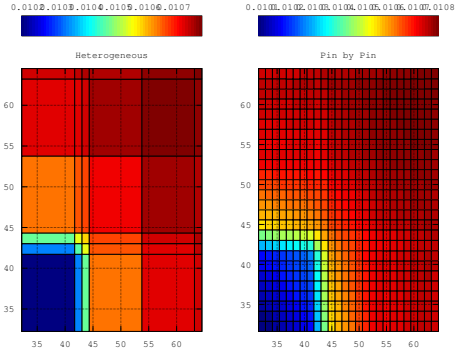

heter. 4x4*

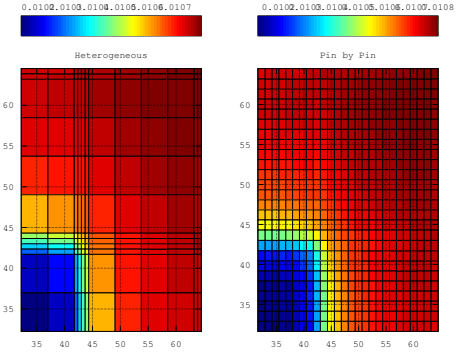

heter. 8x8* (1)

(1) 'het1' mixtures are used

FIGURE 10 – Transport vs diffusion flux distribution of the cluster, case 5

However, the comparison between the different approaches will only be discussed in Section 4. Only the verification of the implementation was looked at in this section.

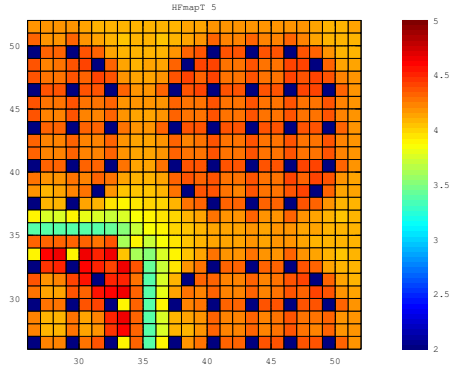

Reference transport pin power distribution

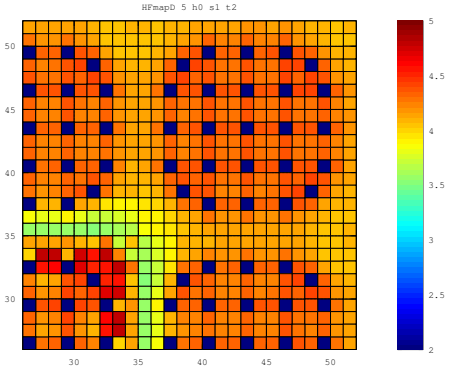

homog. 4x4

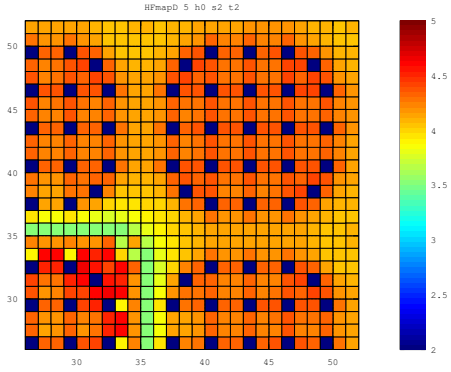

homog. 8x8

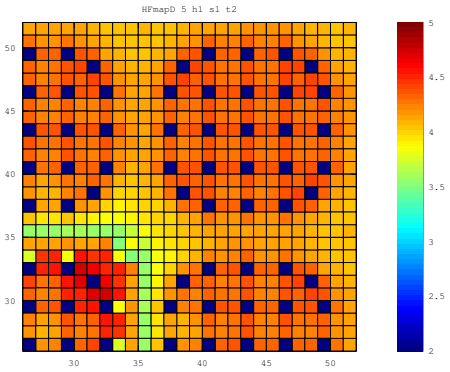

heter. 4x4*

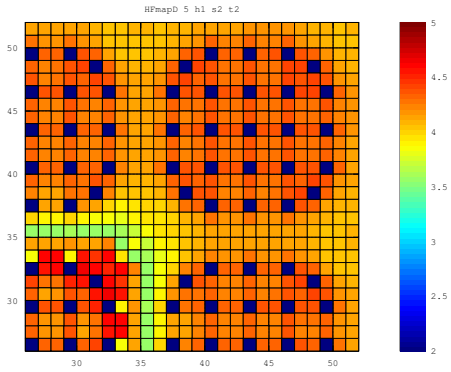

heter. 8x8* (1)

(1) 'heter1' mixtures are used

FIGURE 11 – Transport vs diffusion pin power distribution of the cluster, case 5

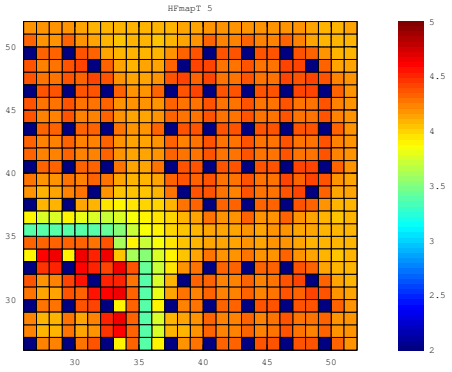

Reference transport pin power distribution

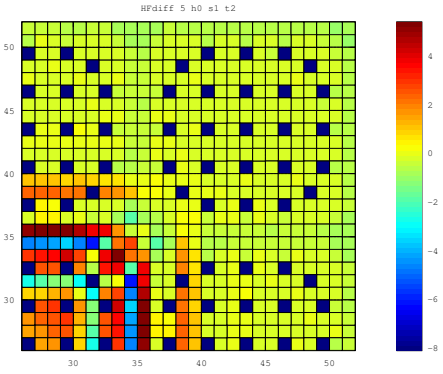

homog. 4x4

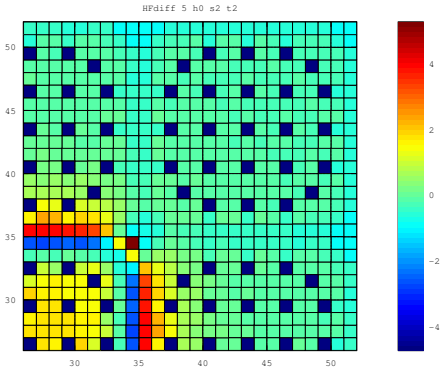

homog. 8x8

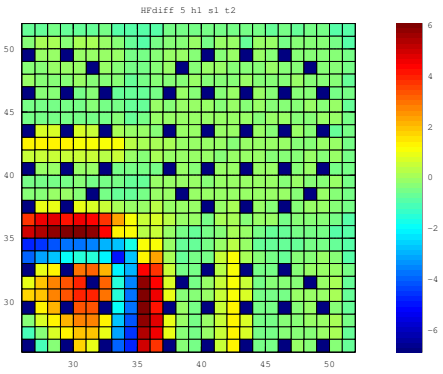

heter. 4x4*

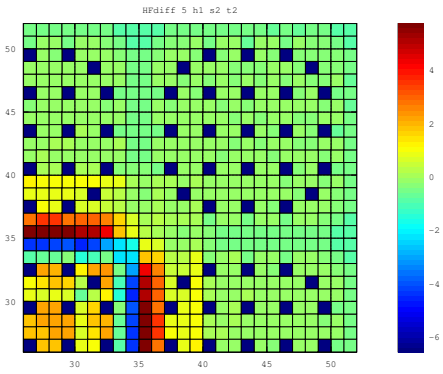

heter. 8x8* (1)

(1) 'heter1' mixtures are used

FIGURE 12 – Relative difference between transport (reference) and diffusion pin power distribution of the cluster, case 5

B Description of input files used as examples and validation tests

Several input files have been generated for the different steps of calculations :
- Step #1 : '*rep900het_mco.x2m*' set
- Step #2 : '*rep900EnrichCOMPO.x2m*' set
- Step #3 : two sets of files '*testNAPGEO.x2m*' and '*rep900cluster.x2m*'
- Validation : '*rep900cluster_mco.x2m*' and '*rep900cluster.x2m*' sets for transport and diffusion calculations respectively.

Most of these input files have been launched many times for the different fuel, heterogeneity level in the assembly homogenization, diffusion mesh splitting, Raviart-Tomas order, interpolation or not, ... To make thing easier / faster and most importantly to reduce the chance of error in all these parameter consistency, most of the computation inputs have been automatically generated and launched using bash scripts. A notification that a bash script was used will be provided in the description of each input file when applicable.

B.1 bash scripts

All the bash scripts used to generate the input files and to launch the calculations are stored at the same level than rdragon or rdongon script. When input file '*main.x2m*' is automatically generated, the corresponding file '*main_template.x2m*' from the folder '*mydata*' is used.

B.2 rep900het_mco.x2m

The main characteristics of this DRAGON-5 data set are the following :
- UOX or MOX assembly
- enrichments are : 7.56%, 4.89% and 2.82% of Pu and 0.25% of U for MOX assembly, and 4% of U for UOX assembly. The MOX pin enrichment are distributed as follows :

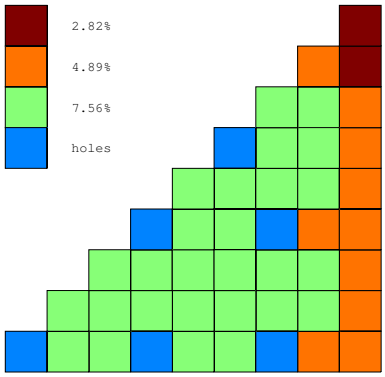

- self-shielding geometry + two levels of geometry for 281 groups and 26 groups,
- burnup until 60GW/t :

1. 71 steps for MOX :
   0.0 9.37499 18.7500 37.5000 74.9999 150.000 325.000 500.000 750.000 1000.00 1500.00 2000.00 2500.00 3000.00 4000.00 5000.00 6000.00 7000.00 8000.00 9000.00 10000.0 11000.0 12000.0 13000.0 14000.0 15000.0 16000.0 17000.0 18000.0 19000.0 20000.0 21000.0 22000.0 23000.0 24000.0 25000.0 26000.0 27000.0 28000.0 29000.0 30000.0 31000.0 32000.0 33000.0 34000.0 35000.0 36000.0 37000.0 38000.0 39000.0 40000.0 41000.0 42000.0 43000.0 44000.0 45000.0 46000.0 47000.0 48000.0 49000.0 50000.0 51000.0 52000.0 53000.0 54000.0 55000.0 56000.0 57000.0 58000.0 59000.0 60000.0

2. 73 steps for UOX :
   0.0 9.37498 18.7500 37.4999 74.9999 150.000 237.500 325.000 412.500 500.000 625.000 750.000 1000.00 1250.00 1500.00 1750.00 2000.00 2500.00 3000.00 3500.00 4000.00 4500.00 5000.00 5500.00 6000.00 6500.00 7000.00 7500.00 8000.00 8500.00 9000.00 9500.00 10000.0 10500.0 11000.0 11500.0 12000.0 12500.0 13000.0 13500.0 14000.0 14500.0 15000.0 15500.0 16000.0 16500.0 17000.0 17500.0 18000.0 18500.0 19000.0 19500.0 20000.0 22000.0 24000.0 26000.0 28000.0 30000.0 32000.0 34000.0 36000.0 38000.0 40000.0 42000.0 44000.0 46000.0 48000.0 50000.0 52000.0 54000.0 56000.0 58000.0 60000.0

– 5 boron steps :
  0.0 600.0 1200.0 1800.0 2400.0
– 1 fuel temperature : 800.0
– 1 coolant temperature : 600.0
– 1 coolant density : 0.659
– Several choices of homogenization :

1. 'Assembly' : homogeneous. Saved in record 'EDI2A'.
2. 'PinByPin' : pin by pin mixtures (45). The water gap is included in the outer pin mixtures. Saved in record 'EDI2B'.
3. 'Heter1' : heterogeneous with 3 mixtures (corner, side and inner parts). The width of the outer mixtures is 1 pin plus the water gap. Saved in record 'EDI2C'.
4. 'Heter2' : Same as 'Heter1', except that the width of the outer mixtures is 2 pins plus the water gap. Saved in record 'EDI2D'.
5. 'Heter3' : Same as 'Heter1', except that the width of the outer mixtures is 3 pins plus the water gap. Saved in record 'EDI2E'.
6. 'All' : all of the above are performed.

– Several choices of homogenization methodology : flux-volume, Selengut, Selengut water gap and Selengut type 'EDF'.

The input file have been created using the bash script : '*allFuel.run.sh*'.

B.3 rep900EnrichCOMPO.x2m

This DONJON-5 set of input file is the following part of the DRAGON '*rep900het_mco.x2m*' in the MULTICOMPO-enrichment process . The main characteristics are then similar to the '*rep900het_mco.x2m'*. Since the MULTICOMPO-enrichment process can be done several times, the $\phi^{\infty}_{i,p}$ names have to be different. As described in the `NAP:` module (See. user guide [10]), a user defined number is associated with each homogenization - projection. In this example, the keyword `IFX` is set to 2 because the 'Heter2' is chosen to get the mixtures properties of the homogenized assembly. We would recommand to use 0 for homogeneous, 1 for 'Heter1', 2 for 'Heter2' and 3 for 'Heter3'. See Sec. A.3 for pictures.

The input file have been created using the bash script : '*allenrich.run.sh*'.

B.4 testNAPGEO.x2m

This DONJON-5 input file has mainly been used during the programation of the `NAP:` module to test all the different features. The reactor described in this set of input files is really small in order to be able to verify the capability in a decent number of data. See Sec. A.2 for picture of the geometry.

The main characteristics are the following :

– 3 types of assemblies
– 3x3 pattern plus coolant all around (top, bottom, side)
– 4 planes along Z-direction (coolant / fuel x 2 / coolant)
– several commented lines either to explain or offer an other option for the input file (usually the automatic way is active and manual way is commented).
– use of partially automatic generation for the geometries

B.5 rep900cluster.x2m

This DONJON-5 input file is very similar to '*testNAPGEO.x2m*' set. See Sec. A.2 for picture of the geometry. Several simulations can be simulated by changing the case number.

The main characteristics are the following :

- 3 types of assemblies (MOX and / or UOX at different burnup)
- 3x3 pattern no coolant
- 1 plane along Z-direction
- several commented lines either to explain or offer an other option for the input file (usually the automatic way is active and manual way is commented).
- use of partially automatic generation for the geometries

The input file have been created using the bash script : '*allClusterDif.run.sh*'.

B.6 rep900cluster_mco.x2m

This DRAGON-5 input set of files is used to validate the pin-power reconstruction. Their purpose is to compute reference pin-power distribution on 3x3 clusters for several cases with transport theory. Results will be compared to the '*rep900cluster.x2m*' diffusion results to validate the methodology and its implementation.

The main characteristics are the following :

- 3 types of assemblies (MOX and / or UOX at different burnup)
- 3x3 pattern infinite domain
- 2D calculations
- isotopic content of each assembly (MOX and UOX) computed with a two previous calls to the '*rep900het_mco.x2m*' set.
- self-shielding and level 1 computations (including condensation at 26 energy groups) performed at assembly level. Final flux calculation is done for the cluster (level 2).

The input file have been created using the bash script : '*allCluster.run.sh*'.

C Results

C.1 Tables results

The final calculations presented below where all performed using interpolation and consistency for the mesh splitting and Raviart-Thomas method during the core and infinite domain flux computations.

The minimum and maximum errors together with the root mean square of the difference between transport and diffusion calculations are presented in Tab. 5 to Tab. 12. The column δ gives the range of error $(max - min)$. Each table corresponds to a different methodology :

1. Flux-Volume normalization of the cross-sections, no Selengut 'STD' : Tab. 5 and 6
2. Selengut normalization of the cross-sections, classical 'SELE_FD' : Tab. 7 and 8
3. Selengut normalization of the cross-sections, macro-calculation water gap 'SELE_MWG' : Tab. 9 and 10
4. Selengut normalization of the cross-sections, 'SELE_EDF' type : Tab. 11 and 12

The range of errors is also presented for all homogenization methods and geometries in Tab. 13 and 14 to facilitate the comparison between the different options.

TABLE 5 – Relative error between reconstruction and transport calculations (%), coarse mesh, STD option in SPH : module

		Pin by Pin				Heterogeneous (het2) 4x4*				Heterogeneous (het1) 4x4*				Homogeneous 4x4			
		min	max	rms	δ	min	max	rms	δ	min	max	rms	δ	min	max	rms	δ
C1	DUAL 2 3	-1.74	3.56	1.25	5.30	-3.42	7.71	1.63	11.14	-3.52	8.51	1.79	12.03	-5.39	13.69	2.27	19.08
	DUAL 3 3	-	-	-	-	-3.42	7.84	1.64	11.26	-2.83	8.71	1.57	11.54	-4.88	17.76	1.90	22.64
C2	DUAL 2 3	-1.98	2.95	1.44	4.93	-3.00	6.78	1.71	9.78	-3.02	7.48	1.84	10.50	-4.33	11.82	2.18	16.15
	DUAL 3 3	-	-	-	-	-2.95	6.89	1.71	9.84	-2.62	7.67	1.69	10.29	-4.50	15.92	1.95	20.41
C3	DUAL 2 3	-1.93	1.39	0.90	3.32	-4.79	3.01	1.33	7.80	-4.50	3.63	1.58	8.13	-6.34	5.70	2.07	12.04
	DUAL 3 3	-	-	-	-	-4.85	3.07	1.32	7.92	-4.78	3.38	1.24	8.16	-8.75	7.63	1.57	16.38
C4	DUAL 2 3	-1.28	1.81	0.99	3.09	-1.49	2.15	1.03	3.64	-1.68	2.52	1.10	4.20	-2.60	3.60	1.20	6.20
	DUAL 3 3	-	-	-	-	-1.36	1.81	1.00	3.16	-1.64	2.07	1.04	3.71	-2.78	3.92	1.18	6.70
C5	DUAL 2 3	-1.06	2.82	0.67	3.88	-2.62	6.55	0.98	9.17	-3.31	7.21	1.16	10.52	-3.89	11.16	1.62	15.06
	DUAL 3 3	-	-	-	-	-2.55	6.66	0.99	9.22	-2.42	7.39	0.97	9.81	-4.29	15.22	1.33	19.51
C6	DUAL 2 3	-5.12	1.72	1.74	6.85	-7.35	2.97	2.11	10.31	-8.61	4.78	2.39	13.39	-8.97	6.66	2.47	15.62
	DUAL 3 3	-	-	-	-	-6.11	1.97	2.07	8.08	-6.71	3.10	1.98	9.80	-8.94	3.37	2.05	12.31
C7	DUAL 2 3	-1.98	2.05	0.75	4.03	-5.97	3.87	1.12	9.84	-6.25	5.66	1.46	11.91	-9.02	7.93	2.24	16.94
	DUAL 3 3	-	-	-	-	-6.07	3.94	1.01	10.01	-6.61	5.03	1.07	11.65	-11.67	10.84	1.73	22.51
C8	DUAL 2 3	-2.63	3.18	1.74	5.81	-4.20	4.79	2.26	8.98	-4.77	6.63	2.61	11.41	-6.01	8.50	3.01	14.51
	DUAL 3 3	-	-	-	-	-4.23	4.10	2.25	8.33	-4.05	5.85	2.17	9.89	-6.85	8.83	2.54	15.69
C9	DUAL 2 3	-0.14	0.15	0.05	0.29	-0.10	0.11	0.04	0.22	-0.10	0.12	0.04	0.22	-0.10	0.12	0.04	0.22
	DUAL 3 3	-	-	-	-	-0.10	0.11	0.04	0.22	-0.10	0.11	0.04	0.22	-0.10	0.12	0.04	0.22
C10	DUAL 2 3	-2.01	1.41	0.92	3.42	-3.08	1.85	1.01	4.94	-3.54	2.29	1.07	5.82	-2.46	1.77	0.98	4.23
	DUAL 3 3	-	-	-	-	-2.30	1.58	0.99	3.88	-2.40	1.71	0.99	4.11	-2.13	1.63	0.96	3.75
C11	DUAL 2 3	-2.07	3.19	1.73	5.26	-3.15	7.11	2.06	10.26	-3.67	7.43	2.20	11.10	-4.49	12.95	2.49	17.44
	DUAL 3 3	-	-	-	-	-3.13	7.19	2.07	10.32	-2.51	7.42	1.99	9.92	-4.18	15.05	2.18	19.24
C12	DUAL 2 3	-0.34	0.35	0.13	0.69	-0.34	0.33	0.12	0.67	-0.37	0.34	0.13	0.71	-0.34	0.33	0.12	0.67
	DUAL 3 3	-	-	-	-	-0.34	0.33	0.12	0.68	-0.33	0.33	0.12	0.67	-0.34	0.33	0.12	0.67

TABLE 6 – Relative error between reconstruction and transport calculations (%), fine mesh, STD option in SPH : module

		Pin by Pin				Heterogeneous (het2) 8x8*				Heterogeneous (het1) 8x8*				Homogeneous 8x8			
		min	max	rms	δ	min	max	rms	δ	min	max	rms	δ	min	max	rms	δ
C1	DUAL 2 3	-1.74	3.56	1.25	5.30	-3.26	7.33	1.54	10.59	-2.82	8.26	1.38	11.08	-4.75	17.27	1.65	22.02
	DUAL 3 3	-	-	-	-	-3.30	7.51	1.56	10.81	-2.79	8.46	1.39	11.25	-4.82	17.29	1.71	22.11
C2	DUAL 2 3	-1.98	2.95	1.44	4.93	-2.81	6.44	1.63	9.25	-2.57	7.26	1.54	9.83	-4.47	15.47	1.78	19.93
	DUAL 3 3	-	-	-	-	-2.85	6.59	1.64	9.44	-2.51	7.44	1.55	9.96	-4.52	15.50	1.82	20.02
C3	DUAL 2 3	-1.93	1.39	0.90	3.32	-4.60	2.82	1.21	7.41	-4.68	3.16	1.08	7.84	-8.40	7.35	1.35	15.74
	DUAL 3 3	-	-	-	-	-4.68	2.90	1.23	7.58	-4.68	3.28	1.03	7.96	-8.47	7.38	1.39	15.84
C4	DUAL 2 3	-1.28	1.81	0.99	3.09	-1.32	1.85	0.99	3.18	-1.70	1.92	1.03	3.62	-2.76	3.88	1.18	6.65
	DUAL 3 3	-	-	-	-	-1.32	1.86	0.99	3.17	-1.62	2.03	1.02	3.66	-2.76	3.88	1.18	6.64
C5	DUAL 2 3	-1.06	2.82	0.67	3.88	-2.41	6.24	0.91	8.65	-2.43	7.00	0.85	9.43	-4.18	14.77	1.15	18.94
	DUAL 3 3	-	-	-	-	-2.45	6.38	0.93	8.83	-2.39	7.18	0.83	9.57	-4.21	14.80	1.19	19.01
C6	DUAL 2 3	-5.12	1.72	1.74	6.85	-5.63	1.93	2.00	7.56	-5.90	3.13	1.81	9.03	-8.51	3.29	1.92	11.80
	DUAL 3 3	-	-	-	-	-5.61	1.95	2.00	7.56	-5.16	1.92	1.79	7.08	-8.60	3.26	1.95	11.87
C7	DUAL 2 3	-1.98	2.05	0.75	4.03	-5.77	3.67	0.98	9.44	-6.45	4.79	1.16	11.24	-11.27	10.58	1.63	21.85
	DUAL 3 3	-	-	-	-	-5.87	3.76	0.97	9.63	-6.49	4.91	0.98	11.40	-11.35	10.59	1.63	21.94
C8	DUAL 2 3	-2.63	3.18	1.74	5.81	-4.07	3.36	2.11	7.43	-3.98	4.89	1.88	8.87	-6.63	8.68	2.24	15.31
	DUAL 3 3	-	-	-	-	-4.12	3.47	2.13	7.59	-3.97	3.84	1.90	7.81	-6.67	8.66	2.31	15.33
C9	DUAL 2 3	-0.14	0.15	0.05	0.29	-0.10	0.11	0.04	0.22	-0.10	0.11	0.04	0.22	-0.10	0.12	0.04	0.22
	DUAL 3 3	-	-	-	-	-0.11	0.12	0.04	0.22	-0.11	0.12	0.04	0.22	-0.10	0.12	0.04	0.22
C10	DUAL 2 3	-2.01	1.41	0.92	3.42	-2.26	1.50	0.96	3.77	-2.25	1.59	0.92	3.84	-2.03	1.45	0.92	3.49
	DUAL 3 3	-	-	-	-	-2.14	1.48	0.96	3.62	-2.07	1.57	0.93	3.64	-2.04	1.51	0.93	3.55
C11	DUAL 2 3	-2.07	3.19	1.73	5.26	-2.99	6.70	1.97	9.69	-2.36	7.00	1.78	9.36	-4.06	14.60	1.95	18.66
	DUAL 3 3	-	-	-	-	-3.03	6.87	1.98	9.90	-2.33	7.18	1.81	9.51	-4.13	14.62	2.01	18.75
C12	DUAL 2 3	-0.34	0.35	0.13	0.69	-0.34	0.33	0.12	0.67	-0.36	0.33	0.13	0.70	-0.34	0.33	0.12	0.67
	DUAL 3 3	-	-	-	-	-0.34	0.33	0.12	0.67	-0.34	0.33	0.12	0.67	-0.34	0.33	0.12	0.67

TABLE 7 – Relative error between reconstruction and transport calculations (%), coarse mesh, SELE_FD option in SPH : module

		Pin by Pin				Heterogeneous (het2) 4x4*				Heterogeneous (het1) 4x4*				Homogeneous 4x4			
		min	max	rms	δ	min	max	rms	δ	min	max	rms	δ	min	max	rms	δ
C1	DUAL 2 3	-6.15	4.99	1.51	11.14	-2.46	3.93	1.35	6.39	-5.48	5.70	1.92	11.17	-7.70	7.15	1.83	14.85
	DUAL 3 3	-	-	-	-	-2.55	3.49	1.31	6.04	-4.88	5.97	1.63	10.85	-2.97	6.62	1.33	9.60
C2	DUAL 2 3	-5.76	4.61	1.67	10.37	-2.54	3.42	1.53	5.96	-4.52	5.13	1.94	9.65	-6.46	6.03	1.81	12.49
	DUAL 3 3	-	-	-	-	-2.42	3.31	1.50	5.73	-4.46	5.50	1.75	9.95	-2.70	5.93	1.50	8.63
C3	DUAL 2 3	-4.40	5.48	1.63	9.88	-3.01	2.51	1.27	5.52	-4.94	5.22	1.97	10.16	-4.89	5.11	1.75	10.00
	DUAL 3 3	-	-	-	-	-3.04	2.52	1.21	5.56	-5.13	4.34	1.65	9.47	-3.03	2.70	1.11	5.72
C4	DUAL 2 3	-1.88	1.75	1.08	3.63	-1.58	2.01	1.01	3.59	-2.17	2.46	1.16	4.63	-1.52	1.84	1.09	3.36
	DUAL 3 3	-	-	-	-	-1.50	1.62	0.99	3.13	-2.11	1.99	1.11	4.10	-1.43	1.86	1.09	3.29
C5	DUAL 2 3	-5.59	5.26	1.25	10.85	-2.45	3.75	0.94	6.19	-4.89	6.06	1.47	10.95	-6.12	5.39	1.31	11.50
	DUAL 3 3	-	-	-	-	-2.24	3.70	0.90	5.94	-4.25	6.16	1.26	10.41	-2.53	5.60	0.89	8.13
C6	DUAL 2 3	-7.37	4.99	1.73	12.36	-6.42	2.64	1.80	9.06	-9.04	6.29	2.33	15.33	-8.86	3.71	2.09	12.58
	DUAL 3 3	-	-	-	-	-6.12	1.77	1.72	7.89	-8.57	2.66	1.87	11.23	-6.09	2.11	1.58	8.20
C7	DUAL 2 3	-5.76	8.31	2.41	14.06	-4.13	4.75	1.69	8.88	-6.37	8.20	2.49	14.57	-5.90	7.42	2.15	13.32
	DUAL 3 3	-	-	-	-	-4.39	4.66	1.61	9.05	-6.80	7.35	2.29	14.15	-4.17	5.13	1.62	9.30
C8	DUAL 2 3	-4.25	3.21	1.90	7.46	-3.09	4.16	1.77	7.25	-5.02	5.67	2.60	10.69	-5.62	4.84	2.37	10.47
	DUAL 3 3	-	-	-	-	-3.05	3.68	1.69	6.73	-4.63	5.13	2.07	9.77	-2.99	3.64	1.68	6.63
C9	DUAL 2 3	-0.14	0.15	0.05	0.29	-0.10	0.11	0.04	0.22	-0.10	0.12	0.04	0.22	-0.10	0.12	0.04	0.22
	DUAL 3 3	-	-	-	-	-0.10	0.11	0.04	0.22	-0.10	0.11	0.04	0.22	-0.10	0.12	0.04	0.22
C10	DUAL 2 3	-1.84	1.31	0.88	3.15	-2.95	1.80	0.97	4.74	-3.45	2.26	1.03	5.71	-2.41	1.84	0.93	4.25
	DUAL 3 3	-	-	-	-	-2.12	1.49	0.95	3.61	-2.24	1.61	0.94	3.85	-1.98	1.54	0.91	3.51
C11	DUAL 2 3	-5.26	4.20	1.77	9.47	-2.76	4.57	1.76	7.33	-4.79	6.03	2.19	10.82	-6.93	7.26	2.09	14.19
	DUAL 3 3	-	-	-	-	-2.50	4.10	1.73	6.60	-3.96	5.73	1.91	9.69	-2.29	5.51	1.70	7.80
C12	DUAL 2 3	-0.34	0.35	0.13	0.69	-0.34	0.33	0.12	0.67	-0.37	0.34	0.13	0.71	-0.34	0.33	0.12	0.67
	DUAL 3 3	-	-	-	-	-0.34	0.33	0.12	0.68	-0.33	0.33	0.12	0.67	-0.34	0.33	0.12	0.67

TABLE 8 – Relative error between reconstruction and transport calculations (%), fine mesh, SELE_FD option in SPH : module

		Pin by Pin				Heterogeneous (het2) 8x8*				Heterogeneous (het1) 8x8*				Homogeneous 8x8			
		min	max	rms	δ	min	max	rms	δ	min	max	rms	δ	min	max	rms	δ
C1	DUAL 2 3	-6.15	4.99	1.51	11.14	-2.95	2.96	1.28	5.91	-5.22	5.73	1.56	10.95	-3.25	6.28	1.25	9.53
	DUAL 3 3	-	-	-	-	-2.63	2.87	1.28	5.51	-4.97	5.68	1.53	10.66	-3.22	6.29	1.26	9.51
C2	DUAL 2 3	-5.76	4.61	1.67	10.37	-2.77	2.82	1.47	5.59	-4.70	5.18	1.68	9.88	-2.94	5.62	1.45	8.56
	DUAL 3 3	-	-	-	-	-2.51	2.72	1.47	5.23	-4.52	5.09	1.66	9.62	-2.90	5.64	1.46	8.54
C3	DUAL 2 3	-4.40	5.48	1.63	9.88	-3.24	2.68	1.22	5.92	-4.81	4.69	1.64	9.51	-3.22	2.91	1.12	6.13
	DUAL 3 3	-	-	-	-	-2.93	2.63	1.20	5.56	-4.77	4.33	1.57	9.10	-3.20	2.86	1.11	6.06
C4	DUAL 2 3	-1.88	1.75	1.08	3.63	-1.36	1.64	0.98	3.00	-2.05	2.03	1.09	4.08	-1.43	1.80	1.08	3.23
	DUAL 3 3	-	-	-	-	-1.34	1.63	0.97	2.97	-2.00	1.97	1.09	3.98	-1.44	1.84	1.08	3.27
C5	DUAL 2 3	-5.59	5.26	1.25	10.85	-2.53	3.56	0.91	6.09	-4.57	5.75	1.25	10.33	-2.73	5.28	0.88	8.01
	DUAL 3 3	-	-	-	-	-2.40	3.47	0.90	5.86	-4.33	5.71	1.21	10.05	-2.72	5.30	0.88	8.02
C6	DUAL 2 3	-7.37	4.99	1.73	12.36	-6.48	2.00	1.69	8.48	-8.01	3.16	1.80	11.17	-6.41	1.51	1.57	7.91
	DUAL 3 3	-	-	-	-	-5.89	1.93	1.68	7.83	-7.86	2.75	1.74	10.60	-6.33	1.48	1.57	7.81
C7	DUAL 2 3	-5.76	8.31	2.41	14.06	-4.35	4.89	1.68	9.24	-6.47	7.55	2.38	14.01	-4.31	5.39	1.75	9.70
	DUAL 3 3	-	-	-	-	-4.02	4.74	1.65	8.77	-6.42	7.34	2.29	13.77	-4.33	5.31	1.71	9.64
C8	DUAL 2 3	-4.25	3.21	1.90	7.46	-3.32	3.08	1.64	6.40	-4.70	3.49	1.95	8.19	-3.19	3.02	1.58	6.22
	DUAL 3 3	-	-	-	-	-3.02	3.01	1.64	6.03	-4.66	3.36	1.90	8.01	-3.18	3.07	1.60	6.25
C9	DUAL 2 3	-0.14	0.15	0.05	0.29	-0.10	0.11	0.04	0.22	-0.10	0.11	0.04	0.22	-0.10	0.12	0.04	0.22
	DUAL 3 3	-	-	-	-	-0.11	0.12	0.04	0.22	-0.11	0.12	0.04	0.22	-0.10	0.12	0.04	0.22
C10	DUAL 2 3	-1.84	1.31	0.88	3.15	-2.08	1.36	0.92	3.44	-2.19	1.62	0.87	3.81	-1.86	1.33	0.86	3.19
	DUAL 3 3	-	-	-	-	-1.96	1.38	0.92	3.34	-1.91	1.48	0.88	3.39	-1.88	1.41	0.88	3.29
C11	DUAL 2 3	-5.26	4.20	1.77	9.47	-2.42	3.32	1.68	5.74	-4.31	4.86	1.79	9.17	-2.58	5.18	1.60	7.76
	DUAL 3 3	-	-	-	-	-2.42	3.29	1.68	5.71	-4.09	4.78	1.78	8.87	-2.54	5.19	1.62	7.73
C12	DUAL 2 3	-0.34	0.35	0.13	0.69	-0.34	0.33	0.12	0.67	-0.35	0.33	0.13	0.69	-0.34	0.33	0.12	0.67
	DUAL 3 3	-	-	-	-	-0.34	0.33	0.12	0.68	-0.34	0.33	0.12	0.67	-0.34	0.33	0.12	0.67

TABLE 9 – Relative error between reconstruction and transport calculations (%), coarse mesh, SELE_MWG option in SPH : module

		Pin by Pin				Heterogeneous (het2) 4x4*				Heterogeneous (het1) 4x4*				Homogeneous 4x4			
		min	max	rms	δ	min	max	rms	δ	min	max	rms	δ	min	max	rms	δ
C1	DUAL 2 3	-1.99	2.48	1.05	4.47	-2.81	8.08	2.21	10.89	-3.64	6.75	1.68	10.39	-2.58	14.84	3.17	17.43
	DUAL 3 3	-	-	-	-	-2.36	7.48	2.24	9.84	-2.02	6.32	1.38	8.34	-2.28	14.76	3.01	17.04
C2	DUAL 2 3	-1.85	2.14	1.32	4.00	-3.04	7.21	2.07	10.25	-2.76	6.21	1.67	8.97	-2.89	13.35	3.05	16.24
	DUAL 3 3	-	-	-	-	-2.46	6.93	2.09	9.39	-2.21	6.13	1.47	8.34	-2.91	13.56	2.97	16.48
C3	DUAL 2 3	-2.38	2.16	0.97	4.53	-4.18	3.48	2.51	7.66	-2.92	3.66	1.83	6.58	-5.79	5.78	3.80	11.57
	DUAL 3 3	-	-	-	-	-4.17	3.42	2.54	7.59	-3.08	3.51	1.57	6.58	-5.26	5.76	3.67	11.02
C4	DUAL 2 3	-1.22	1.71	1.00	2.93	-0.97	1.36	0.52	2.33	-1.44	2.19	0.90	3.63	-2.69	2.93	0.53	5.62
	DUAL 3 3	-	-	-	-	-0.81	0.95	0.45	1.77	-1.27	1.44	0.83	2.71	-2.69	3.00	0.51	5.68
C5	DUAL 2 3	-1.71	2.81	0.73	4.52	-1.51	6.75	1.74	8.25	-2.91	5.59	1.32	8.49	-2.43	12.38	2.77	14.80
	DUAL 3 3	-	-	-	-	-1.51	6.45	1.77	7.96	-1.36	5.41	1.16	6.77	-1.69	12.91	2.71	14.60
C6	DUAL 2 3	-5.44	1.94	1.48	7.38	-9.36	3.33	2.60	12.69	-7.96	4.76	2.31	12.72	-9.56	4.86	3.18	14.42
	DUAL 3 3	-	-	-	-	-8.57	2.60	2.58	11.17	-6.99	2.90	1.87	9.88	-9.03	3.01	2.93	12.04
C7	DUAL 2 3	-2.85	3.85	1.45	6.70	-4.15	2.10	1.75	6.25	-3.55	4.91	1.47	8.46	-7.92	5.91	3.82	13.83
	DUAL 3 3	-	-	-	-	-4.14	1.97	1.75	6.11	-4.03	3.34	1.25	7.37	-8.16	7.71	3.70	15.88
C8	DUAL 2 3	-2.38	2.82	1.44	5.20	-4.87	5.63	3.05	10.50	-4.22	6.18	2.60	10.40	-5.93	7.72	4.19	13.65
	DUAL 3 3	-	-	-	-	-4.58	5.02	3.07	9.59	-3.78	5.58	2.15	9.36	-5.13	6.40	3.99	11.53
C9	DUAL 2 3	-0.15	0.14	0.05	0.29	-0.12	0.15	0.04	0.26	-0.13	0.14	0.05	0.27	-0.15	0.18	0.07	0.34
	DUAL 3 3	-	-	-	-	-0.11	0.14	0.04	0.25	-0.13	0.14	0.05	0.27	-0.15	0.18	0.07	0.34
C10	DUAL 2 3	-1.75	1.28	0.81	3.04	-2.93	1.72	0.90	4.65	-2.72	2.27	0.78	4.99	-1.92	1.89	0.53	3.81
	DUAL 3 3	-	-	-	-	-2.17	1.45	0.87	3.63	-1.56	1.09	0.59	2.65	-1.37	1.22	0.42	2.59
C11	DUAL 2 3	-1.88	2.68	1.46	4.56	-3.32	8.37	2.42	11.68	-3.19	7.29	1.90	10.48	-3.04	13.72	3.04	16.76
	DUAL 3 3	-	-	-	-	-2.68	7.74	2.44	10.42	-2.05	6.79	1.57	8.84	-2.50	12.18	2.86	14.69
C12	DUAL 2 3	-0.35	0.36	0.13	0.71	-0.37	0.43	0.15	0.80	-0.49	0.35	0.15	0.84	-0.22	0.31	0.10	0.52
	DUAL 3 3	-	-	-	-	-0.37	0.42	0.15	0.79	-0.42	0.34	0.15	0.77	-0.22	0.31	0.10	0.52

TABLE 10 – Relative error between reconstruction and transport calculations (%), fine mesh, SELE_MWG option in SPH : module

		Pin by Pin				Heterogeneous (het2) 8x8*				Heterogeneous (het1) 8x8*				Homogeneous 8x8			
		min	max	rms	δ	min	max	rms	δ	min	max	rms	δ	min	max	rms	δ
C1	DUAL 2 3	-1.99	2.48	1.05	4.47	-2.42	6.77	2.16	9.19	-2.42	5.55	1.23	7.97	-2.15	14.39	2.81	16.54
	DUAL 3 3	-	-	-	-	-2.26	6.62	2.17	8.89	-2.08	4.08	1.22	6.16	-2.20	14.40	2.87	16.60
C2	DUAL 2 3	-1.85	2.14	1.32	4.00	-2.51	6.04	2.02	8.55	-1.78	5.06	1.34	6.85	-2.77	13.23	2.82	16.00
	DUAL 3 3	-	-	-	-	-2.42	6.19	2.03	8.61	-1.74	4.14	1.35	5.88	-2.81	13.25	2.86	16.06
C3	DUAL 2 3	-2.38	2.16	0.97	4.53	-4.14	2.97	2.47	7.11	-2.71	2.47	1.45	5.18	-5.21	5.62	3.55	10.83
	DUAL 3 3	-	-	-	-	-4.15	2.95	2.48	7.10	-2.67	2.06	1.43	4.73	-5.22	5.64	3.58	10.87
C4	DUAL 2 3	-1.22	1.71	1.00	2.93	-0.90	0.98	0.44	1.89	-1.23	1.46	0.81	2.69	-2.69	2.99	0.51	5.68
	DUAL 3 3	-	-	-	-	-0.87	0.98	0.43	1.85	-1.18	1.44	0.80	2.62	-2.69	2.99	0.51	5.68
C5	DUAL 2 3	-1.71	2.81	0.73	4.52	-1.51	5.59	1.72	7.10	-1.74	4.46	1.06	6.19	-1.66	12.58	2.57	14.24
	DUAL 3 3	-	-	-	-	-1.51	5.81	1.73	7.32	-1.42	3.71	1.06	5.13	-1.67	12.60	2.61	14.27
C6	DUAL 2 3	-5.44	1.94	1.48	7.38	-8.16	2.60	2.52	10.76	-6.39	2.42	1.75	8.81	-8.95	2.46	2.87	11.41
	DUAL 3 3	-	-	-	-	-8.07	2.60	2.52	10.67	-6.21	1.83	1.71	8.05	-8.93	2.43	2.88	11.36
C7	DUAL 2 3	-2.85	3.85	1.45	6.70	-4.10	1.89	1.72	5.99	-3.64	3.58	1.25	7.22	-7.87	7.52	3.60	15.39
	DUAL 3 3	-	-	-	-	-4.11	1.91	1.72	6.02	-3.60	3.32	1.16	6.92	-7.93	7.53	3.62	15.46
C8	DUAL 2 3	-2.38	2.82	1.44	5.20	-4.24	4.22	2.96	8.46	-2.86	4.10	1.92	6.96	-4.97	6.29	3.79	11.25
	DUAL 3 3	-	-	-	-	-4.21	4.31	2.98	8.52	-2.83	3.56	1.92	6.39	-5.04	6.26	3.84	11.30
C9	DUAL 2 3	-0.15	0.14	0.05	0.29	-0.12	0.15	0.04	0.27	-0.13	0.14	0.05	0.27	-0.15	0.18	0.07	0.34
	DUAL 3 3	-	-	-	-	-0.12	0.14	0.04	0.26	-0.13	0.14	0.05	0.27	-0.15	0.18	0.07	0.34
C10	DUAL 2 3	-1.75	1.28	0.81	3.04	-2.16	1.32	0.85	3.48	-1.43	1.09	0.54	2.52	-1.42	1.30	0.40	2.72
	DUAL 3 3	-	-	-	-	-2.02	1.35	0.85	3.37	-1.23	1.09	0.53	2.32	-1.40	1.28	0.41	2.68
C11	DUAL 2 3	-1.88	2.68	1.46	4.56	-2.78	6.93	2.35	9.72	-1.96	5.91	1.40	7.87	-2.44	11.84	2.68	14.27
	DUAL 3 3	-	-	-	-	-2.57	6.86	2.36	9.43	-1.67	4.47	1.41	6.15	-2.44	11.85	2.73	14.28
C12	DUAL 2 3	-0.35	0.36	0.13	0.71	-0.37	0.43	0.15	0.80	-0.43	0.35	0.15	0.78	-0.22	0.31	0.10	0.53
	DUAL 3 3	-	-	-	-	-0.37	0.43	0.15	0.80	-0.43	0.35	0.15	0.77	-0.22	0.31	0.10	0.52

TABLE 11 – Relative error between reconstruction and transport calculations (%), coarse mesh, SELE_EDF option in SPH : module

		Pin by Pin				Heterogeneous (het2) 4x4*				Heterogeneous (het1) 4x4*				Homogeneous 4x4			
		min	max	rms	δ	min	max	rms	δ	min	max	rms	δ	min	max	rms	δ
C1	DUAL 2 3	-1.71	2.18	1.02	3.89	-2.43	7.01	1.84	9.44	-4.43	5.63	1.62	10.06	-2.77	15.76	3.42	18.53
	DUAL 3 3	-	-	-	-	-1.96	6.42	1.86	8.39	-2.51	5.07	1.28	7.58	-2.45	15.72	3.29	18.17
C2	DUAL 2 3	-1.88	2.09	1.34	3.96	-2.87	6.24	1.83	9.10	-3.66	4.78	1.73	8.45	-2.95	13.99	3.25	16.94
	DUAL 3 3	-	-	-	-	-2.27	5.98	1.85	8.26	-2.25	4.55	1.51	6.79	-2.96	14.21	3.18	17.17
C3	DUAL 2 3	-2.19	1.95	0.91	4.13	-3.48	3.02	2.05	6.50	-2.89	4.39	1.53	7.28	-6.11	6.04	4.10	12.15
	DUAL 3 3	-	-	-	-	-3.47	2.97	2.07	6.44	-2.97	2.89	1.08	5.86	-5.61	6.24	3.99	11.86
C4	DUAL 2 3	-1.25	1.78	1.00	3.02	-0.91	1.23	0.47	2.15	-1.67	2.53	1.10	4.20	-2.97	3.16	0.67	6.13
	DUAL 3 3	-	-	-	-	-0.93	0.88	0.39	1.80	-1.27	1.79	1.05	3.07	-2.97	3.23	0.66	6.20
C5	DUAL 2 3	-1.48	2.56	0.68	4.05	-1.30	5.80	1.44	7.10	-4.00	4.27	1.11	8.27	-2.48	13.09	2.99	15.57
	DUAL 3 3	-	-	-	-	-1.30	5.52	1.47	6.82	-2.00	3.93	0.83	5.93	-1.77	13.65	2.94	15.41
C6	DUAL 2 3	-5.30	1.66	1.48	6.96	-8.42	3.13	2.31	11.55	-7.39	5.15	2.18	12.54	-9.92	4.93	3.29	14.85
	DUAL 3 3	-	-	-	-	-7.54	2.16	2.28	9.70	-6.57	2.79	1.68	9.36	-9.40	3.08	3.06	12.48
C7	DUAL 2 3	-2.58	3.62	1.41	6.20	-3.26	1.65	1.30	4.91	-3.21	6.60	1.77	9.81	-8.45	6.18	4.18	14.64
	DUAL 3 3	-	-	-	-	-3.25	1.59	1.27	4.83	-3.69	3.93	1.42	7.62	-8.63	8.02	4.09	16.65
C8	DUAL 2 3	-2.25	2.84	1.43	5.09	-4.26	5.03	2.60	9.29	-4.52	5.98	2.35	10.50	-6.12	7.98	4.39	14.10
	DUAL 3 3	-	-	-	-	-3.98	4.46	2.61	8.43	-3.26	5.32	1.76	8.58	-5.37	6.64	4.20	12.01
C9	DUAL 2 3	-0.14	0.15	0.05	0.29	-0.11	0.11	0.04	0.22	-0.10	0.12	0.04	0.22	-0.17	0.20	0.08	0.37
	DUAL 3 3	-	-	-	-	-0.11	0.10	0.04	0.21	-0.10	0.11	0.04	0.22	-0.17	0.20	0.08	0.37
C10	DUAL 2 3	-1.79	1.32	0.83	3.11	-2.67	1.59	0.81	4.26	-3.27	2.18	1.01	5.46	-1.94	2.02	0.52	3.96
	DUAL 3 3	-	-	-	-	-1.90	1.32	0.79	3.22	-2.19	1.61	0.91	3.80	-1.40	1.35	0.40	2.75
C11	DUAL 2 3	-1.91	2.65	1.47	4.56	-2.95	7.14	2.03	10.09	-4.09	6.24	1.99	10.33	-3.20	14.37	3.22	17.57
	DUAL 3 3	-	-	-	-	-2.30	6.54	2.04	8.84	-2.17	5.61	1.69	7.79	-2.65	12.83	3.06	15.48
C12	DUAL 2 3	-0.34	0.35	0.13	0.69	-0.22	0.31	0.10	0.53	-0.37	0.34	0.13	0.71	-0.22	0.31	0.10	0.53
	DUAL 3 3	-	-	-	-	-0.23	0.31	0.10	0.54	-0.33	0.33	0.12	0.67	-0.22	0.31	0.10	0.53

TABLE 12 – Relative error between reconstruction and transport calculations (%), fine mesh, SELE_EDF option in SPH : module

		Pin by Pin				Heterogeneous (het2) 8x8*				Heterogeneous (het1) 8x8*				Homogeneous 8x8			
		min	max	rms	δ	min	max	rms	δ	min	max	rms	δ	min	max	rms	δ
C1	DUAL 2 3	-1.71	2.18	1.02	3.89	-2.03	5.73	1.78	7.76	-2.93	4.54	1.16	7.47	-2.32	15.34	3.09	17.67
	DUAL 3 3	-	-	-	-	-1.87	5.56	1.79	7.43	-2.57	3.27	1.12	5.84	-2.37	15.35	3.14	17.72
C2	DUAL 2 3	-1.88	2.09	1.34	3.96	-2.31	5.19	1.78	7.50	-2.56	3.72	1.41	6.28	-2.81	13.88	3.03	16.69
	DUAL 3 3	-	-	-	-	-2.23	5.24	1.78	7.47	-2.28	2.96	1.39	5.24	-2.86	13.89	3.07	16.75
C3	DUAL 2 3	-2.19	1.95	0.91	4.13	-3.44	2.49	2.00	5.93	-2.61	2.56	1.03	5.17	-5.56	6.10	3.87	11.67
	DUAL 3 3	-	-	-	-	-3.45	2.49	2.01	5.94	-2.56	2.15	0.92	4.71	-5.58	6.13	3.90	11.70
C4	DUAL 2 3	-1.25	1.78	1.00	3.02	-0.91	0.90	0.38	1.81	-1.36	1.84	1.03	3.20	-2.97	3.23	0.66	6.20
	DUAL 3 3	-	-	-	-	-0.91	0.90	0.38	1.82	-1.24	1.80	1.02	3.04	-2.97	3.22	0.66	6.19
C5	DUAL 2 3	-1.48	2.56	0.68	4.05	-1.29	4.75	1.41	6.05	-2.40	3.23	0.78	5.63	-1.73	13.30	2.80	15.03
	DUAL 3 3	-	-	-	-	-1.30	4.88	1.42	6.17	-2.05	3.01	0.73	5.06	-1.74	13.32	2.84	15.07
C6	DUAL 2 3	-5.30	1.66	1.48	6.96	-7.09	2.13	2.22	9.22	-5.97	2.49	1.56	8.45	-9.32	2.53	2.99	11.85
	DUAL 3 3	-	-	-	-	-7.02	2.13	2.23	9.15	-5.79	1.72	1.51	7.51	-9.30	2.51	3.01	11.81
C7	DUAL 2 3	-2.58	3.62	1.41	6.20	-3.20	1.47	1.24	4.68	-3.29	4.62	1.55	7.91	-8.35	7.83	3.99	16.17
	DUAL 3 3	-	-	-	-	-3.22	1.48	1.24	4.70	-3.25	3.90	1.40	7.15	-8.40	7.83	4.01	16.24
C8	DUAL 2 3	-2.25	2.84	1.43	5.09	-3.58	3.76	2.50	7.34	-2.69	3.94	1.56	6.63	-5.20	6.52	4.01	11.73
	DUAL 3 3	-	-	-	-	-3.59	3.74	2.52	7.34	-2.64	3.26	1.51	5.91	-5.27	6.50	4.06	11.77
C9	DUAL 2 3	-0.14	0.15	0.05	0.29	-0.11	0.10	0.04	0.21	-0.10	0.11	0.04	0.22	-0.17	0.20	0.08	0.37
	DUAL 3 3	-	-	-	-	-0.11	0.11	0.04	0.22	-0.11	0.12	0.04	0.22	-0.17	0.20	0.08	0.37
C10	DUAL 2 3	-1.79	1.32	0.83	3.11	-1.86	1.24	0.76	3.10	-2.04	1.44	0.84	3.49	-1.44	1.43	0.39	2.87
	DUAL 3 3	-	-	-	-	-1.74	1.22	0.76	2.96	-1.85	1.48	0.85	3.33	-1.42	1.41	0.39	2.84
C11	DUAL 2 3	-1.91	2.65	1.47	4.56	-2.40	5.74	1.95	8.14	-2.52	4.92	1.53	7.44	-2.61	12.48	2.87	15.09
	DUAL 3 3	-	-	-	-	-2.20	5.65	1.96	7.85	-2.15	3.30	1.52	5.45	-2.59	12.49	2.92	15.08
C12	DUAL 2 3	-0.34	0.35	0.13	0.69	-0.22	0.31	0.10	0.53	-0.35	0.33	0.13	0.69	-0.23	0.31	0.10	0.53
	DUAL 3 3	-	-	-	-	-0.22	0.31	0.10	0.53	-0.34	0.33	0.12	0.67	-0.22	0.31	0.10	0.53

TABLE 13 – Range of relative error δ between reconstruction and transport calculations for all options, coarse mesh (%)

		Pin by Pin				Heterogeneous (het2) 4x4*				Heterogeneous (het1) 4x4*				Homogeneous 4x4			
		STD	SELE_FD	SELE_MWG	SELE_EDF	STD	SELE_FD	SELE_MWG	SELE_EDF	STD	SELE_FD	SELE_MWG	SELE_EDF	STD	SELE_FD	SELE_MWG	SELE_EDF
C1	DUAL 2 3	5.30	11.14	4.47	3.89	11.14	6.39	10.89	9.44	12.03	11.17	10.39	10.06	19.08	14.85	17.43	18.53
	DUAL 3 3	-	-	-	-	11.26	6.04	9.84	8.39	11.54	10.85	8.34	7.58	22.64	9.60	17.04	18.17
C2	DUAL 2 3	4.93	10.37	4.00	3.96	9.78	5.96	10.25	9.10	10.50	9.65	8.97	8.45	16.15	12.49	16.24	16.94
	DUAL 3 3	-	-	-	-	9.84	5.73	9.39	8.26	10.29	9.95	8.34	6.79	20.41	8.63	16.48	17.17
C3	DUAL 2 3	3.32	9.88	4.53	4.13	7.80	5.52	7.66	6.50	8.13	10.16	6.58	7.28	12.04	10.00	11.57	12.15
	DUAL 3 3	-	-	-	-	7.92	5.56	7.59	6.44	8.16	9.47	6.58	5.86	16.38	5.72	11.02	11.86
C4	DUAL 2 3	3.09	3.63	2.93	3.02	3.64	3.59	2.33	2.15	4.20	4.63	3.63	4.20	6.20	3.36	5.62	6.13
	DUAL 3 3	-	-	-	-	3.16	3.13	1.77	1.80	3.71	4.10	2.71	3.07	6.70	3.29	5.68	6.20
C5	DUAL 2 3	3.88	10.85	4.52	4.05	9.17	6.19	8.25	7.10	10.52	10.95	8.49	8.27	15.06	11.50	14.80	15.57
	DUAL 3 3	-	-	-	-	9.22	5.94	7.96	6.82	9.81	10.41	6.77	5.93	19.51	8.13	14.60	15.41
C6	DUAL 2 3	6.85	12.36	7.38	6.96	10.31	9.06	12.69	11.55	13.39	15.33	12.72	12.54	15.62	12.58	14.42	14.85
	DUAL 3 3	-	-	-	-	8.08	7.89	11.17	9.70	9.80	11.23	9.88	9.36	12.31	8.20	12.04	12.48
C7	DUAL 2 3	4.03	14.06	6.70	6.20	9.84	8.88	6.25	4.91	11.91	14.57	8.46	9.81	16.94	13.32	13.83	14.64
	DUAL 3 3	-	-	-	-	10.01	9.05	6.11	4.83	11.65	14.15	7.37	7.62	22.51	9.30	15.88	16.65
C8	DUAL 2 3	5.81	7.46	5.20	5.09	8.98	7.25	10.50	9.29	11.41	10.69	10.40	10.50	14.51	10.47	13.65	14.10
	DUAL 3 3	-	-	-	-	8.33	6.73	9.59	8.43	9.89	9.77	9.36	8.58	15.69	6.63	11.53	12.01
C9	DUAL 2 3	0.29	0.29	0.29	0.29	0.22	0.22	0.26	0.22	0.22	0.22	0.27	0.22	0.22	0.22	0.34	0.37
	DUAL 3 3	-	-	-	-	0.22	0.22	0.25	0.21	0.22	0.22	0.27	0.22	0.22	0.22	0.34	0.37
C10	DUAL 2 3	3.42	3.15	3.04	3.11	4.94	4.74	4.65	4.26	5.82	5.71	4.99	5.46	4.23	4.25	3.81	3.96
	DUAL 3 3	-	-	-	-	3.88	3.61	3.63	3.22	4.11	3.85	2.65	3.80	3.75	3.51	2.59	2.75
C11	DUAL 2 3	5.26	9.47	4.56	4.56	10.26	7.33	11.68	10.09	11.10	10.82	10.48	10.33	17.44	14.19	16.76	17.57
	DUAL 3 3	-	-	-	-	10.32	6.60	10.42	8.84	9.92	9.69	8.84	7.79	19.24	7.80	14.69	15.48
C12	DUAL 2 3	0.69	0.69	0.71	0.69	0.67	0.67	0.80	0.53	0.71	0.71	0.84	0.71	0.67	0.67	0.52	0.53
	DUAL 3 3	-	-	-	-	0.68	0.68	0.79	0.54	0.67	0.67	0.77	0.67	0.67	0.67	0.52	0.53

TABLE 14 – Range of relative error δ between reconstruction and transport calculations for all options, fine mesh (%)

		Pin by Pin				Heterogeneous (het2) 8x8*				Heterogeneous (het1) 8x8*				Homogeneous 8x8			
		STD	SELE_FD	SELE_MWG	SELE_EDF	STD	SELE_FD	SELE_MWG	SELE_EDF	STD	SELE_FD	SELE_MWG	SELE_EDF	STD	SELE_FD	SELE_MWG	SELE_EDF
C1	DUAL 2 3	5.30	11.14	4.47	3.89	10.59	5.91	9.19	7.76	11.08	10.95	7.97	7.47	22.02	9.53	16.54	17.67
	DUAL 3 3	-	-	-	-	10.81	5.51	8.89	7.43	11.25	10.66	6.16	5.84	22.11	9.51	16.60	17.72
C2	DUAL 2 3	4.93	10.37	4.00	3.96	9.25	5.59	8.55	7.50	9.83	9.88	6.85	6.28	19.93	8.56	16.00	16.69
	DUAL 3 3	-	-	-	-	9.44	5.23	8.61	7.47	9.96	9.62	5.88	5.24	20.02	8.54	16.06	16.75
C3	DUAL 2 3	3.32	9.88	4.53	4.13	7.41	5.92	7.11	5.93	7.84	9.51	5.18	5.17	15.74	6.13	10.83	11.67
	DUAL 3 3	-	-	-	-	7.58	5.56	7.10	5.94	7.96	9.10	4.73	4.71	15.84	6.06	10.87	11.70
C4	DUAL 2 3	3.09	3.63	2.93	3.02	3.18	3.00	1.89	1.81	3.62	4.08	2.69	3.20	6.65	3.23	5.68	6.20
	DUAL 3 3	-	-	-	-	3.17	2.97	1.85	1.82	3.66	3.98	2.62	3.04	6.64	3.27	5.68	6.19
C5	DUAL 2 3	3.88	10.85	4.52	4.05	8.65	6.09	7.10	6.05	9.43	10.33	6.19	5.63	18.94	8.01	14.24	15.03
	DUAL 3 3	-	-	-	-	8.83	5.86	7.32	6.17	9.57	10.05	5.13	5.06	19.01	8.02	14.27	15.07
C6	DUAL 2 3	6.85	12.36	7.38	6.96	7.56	8.48	10.76	9.22	9.03	11.17	8.81	8.45	11.80	7.91	11.41	11.85
	DUAL 3 3	-	-	-	-	7.56	7.83	10.67	9.15	7.08	10.60	8.05	7.51	11.87	7.81	11.36	11.81
C7	DUAL 2 3	4.03	14.06	6.70	6.20	9.44	9.24	5.99	4.68	11.24	14.01	7.22	7.91	21.85	9.70	15.39	16.17
	DUAL 3 3	-	-	-	-	9.63	8.77	6.02	4.70	11.40	13.77	6.92	7.15	21.94	9.64	15.46	16.24
C8	DUAL 2 3	5.81	7.46	5.20	5.09	7.43	6.40	8.46	7.34	8.87	8.19	6.96	6.63	15.31	6.22	11.25	11.73
	DUAL 3 3	-	-	-	-	7.59	6.03	8.52	7.34	7.81	8.01	6.39	5.91	15.33	6.25	11.30	11.77
C9	DUAL 2 3	0.29	0.29	0.29	0.29	0.22	0.22	0.27	0.21	0.22	0.22	0.27	0.22	0.22	0.22	0.34	0.37
	DUAL 3 3	-	-	-	-	0.22	0.22	0.26	0.22	0.22	0.22	0.27	0.22	0.22	0.22	0.34	0.37
C10	DUAL 2 3	3.42	3.15	3.04	3.11	3.77	3.44	3.48	3.10	3.84	3.81	2.52	3.49	3.49	3.19	2.72	2.87
	DUAL 3 3	-	-	-	-	3.62	3.34	3.37	2.96	3.64	3.39	2.32	3.33	3.55	3.29	2.68	2.84
C11	DUAL 2 3	5.26	9.47	4.56	4.56	9.69	5.74	9.72	8.14	9.36	9.17	7.87	7.44	18.66	7.76	14.27	15.09
	DUAL 3 3	-	-	-	-	9.90	5.71	9.43	7.85	9.51	8.87	6.15	5.45	18.75	7.73	14.28	15.08
C12	DUAL 2 3	0.69	0.69	0.71	0.69	0.67	0.67	0.80	0.53	0.70	0.69	0.78	0.69	0.67	0.67	0.53	0.53
	DUAL 3 3	-	-	-	-	0.67	0.68	0.80	0.53	0.67	0.67	0.77	0.67	0.67	0.67	0.52	0.53

C.2 Figure results

The distribution of the error for 4x4* homogenization with 'DUAL 3 3' tracking is presented for all SPH method for all configurations in Fig. 13 to 16.

C1 M0-U0-U20

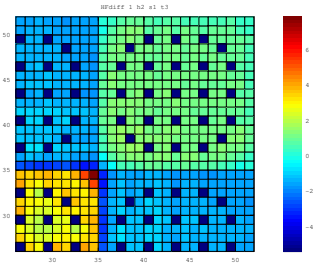

C2 M20-U10-U60

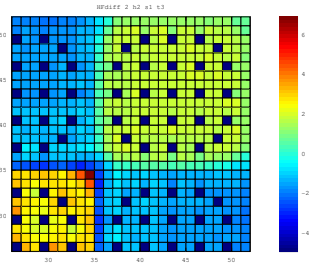

C3 M10-M30-U20

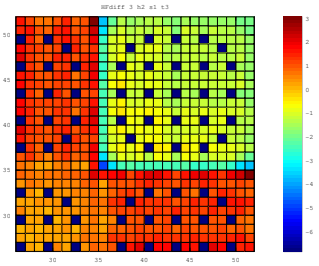

C4 M20-M50-M0

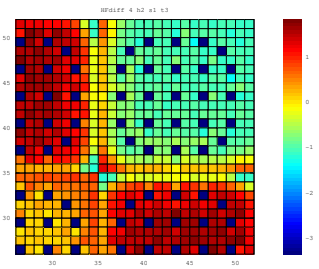

C5 M20-U20-U20

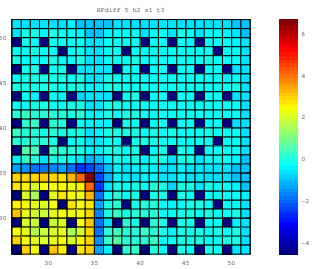

C6 U0-M30-M30

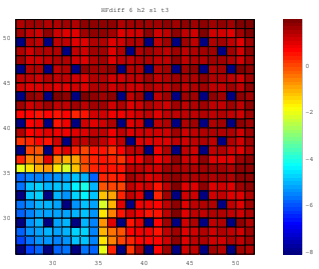

C7 M0-M0-U60

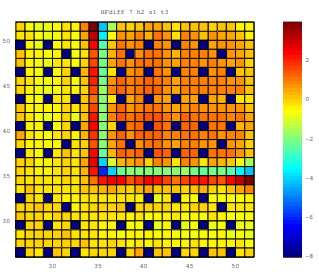

C8 M60-U10-M40

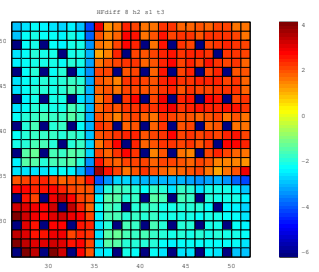

C9 U12-U12-U12

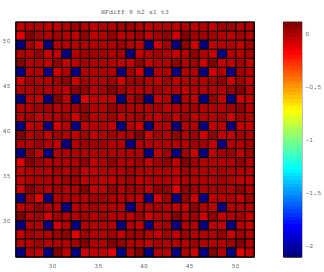

C10 U0-U36-U12

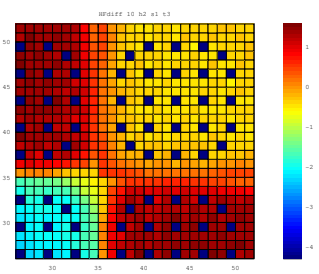

C11 M20-U0-U40

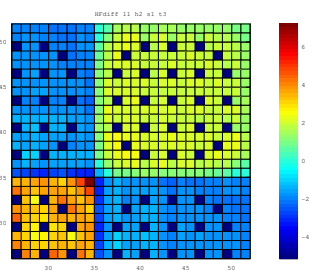

C12 M12-M12-M12

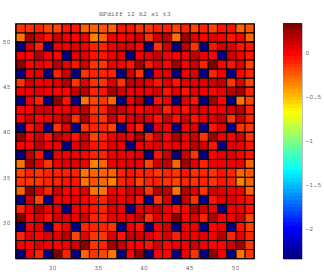

FIGURE 13 – Transport vs diffusion pin power distribution of all clusters shpnew STD

C1 M0-U0-U20

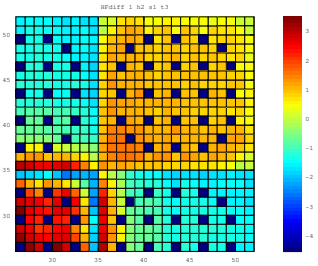

C2 M20-U10-U60

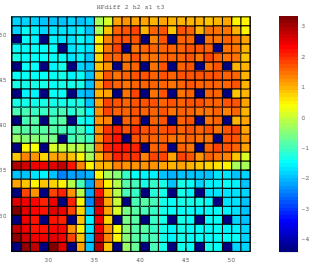

C3 M10-M30-U20

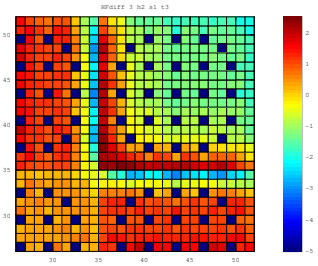

C4 M20-M50-M0

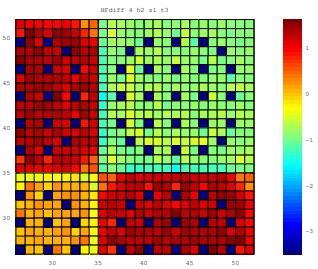

C5 M20-U20-U20

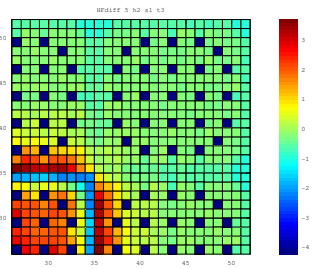

C6 U0-M30-M30

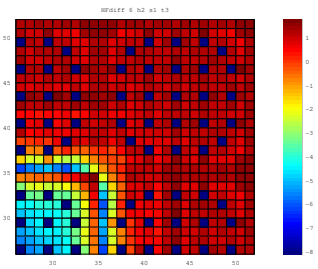

C7 M0-M0-U60

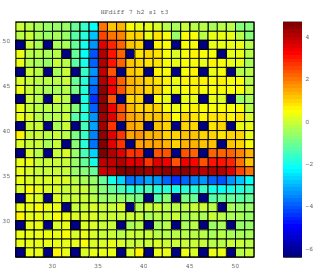

C8 M60-U10-M40

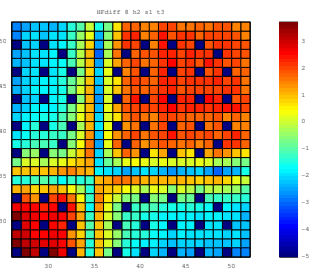

C9 U12-U12-U12

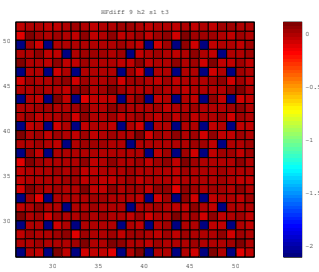

C10 U0-U36-U12

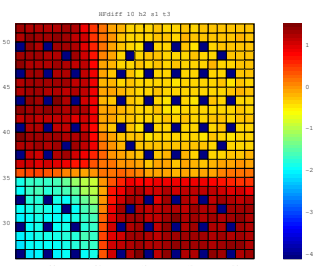

C11 M20-U0-U40

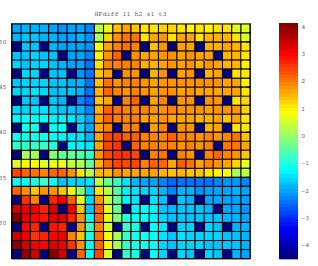

C12 M12-M12-M12

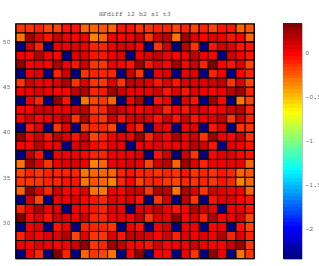

FIGURE 14 – Transport vs diffusion pin power distribution of all clusters shpnew SELE_FD

C1 M0-U0-U20

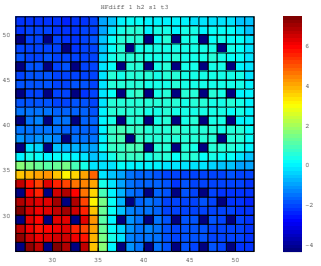

C2 M20-U10-U60

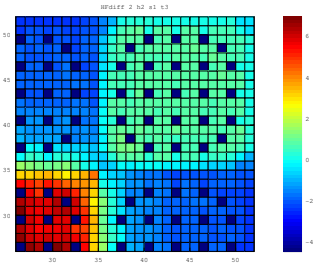

C3 M10-M30-U20

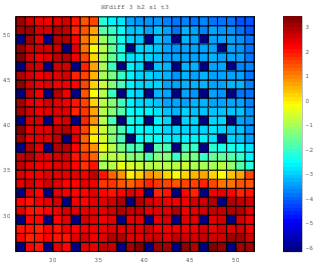

C4 M20-M50-M0

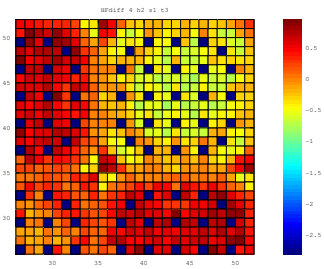

C5 M20-U20-U20

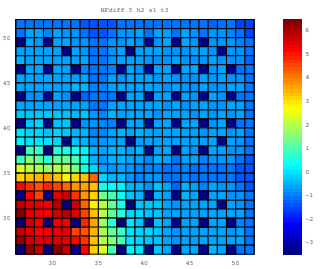

C6 U0-M30-M30

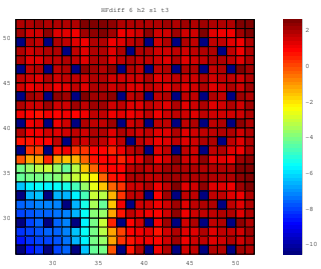

C7 M0-M0-U60

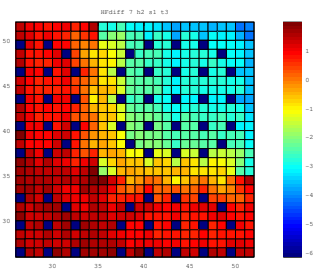

C8 M60-U10-M40

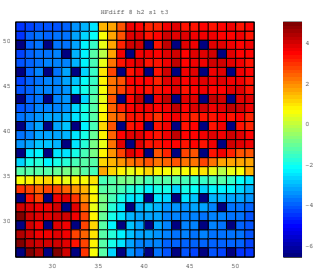

C9 U12-U12-U12

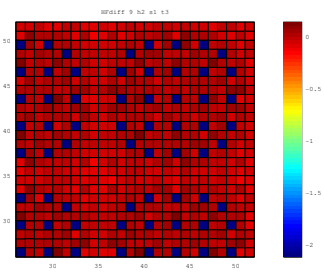

C10 U0-U36-U12

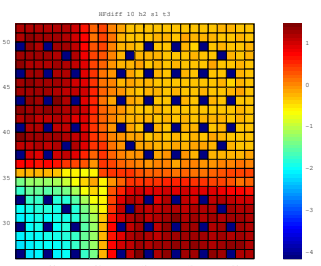

C11 M20-U0-U40

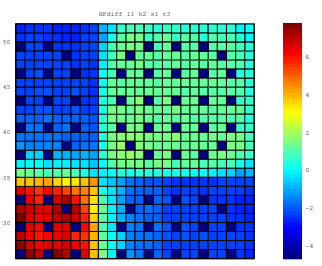

C12 M12-M12-M12

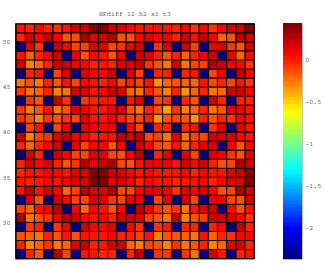

FIGURE 15 – Transport vs diffusion pin power distribution of all clusters shpnew SELE_MWG

C1 M0-U0-U20

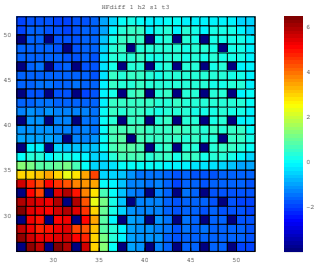

C2 M20-U10-U60

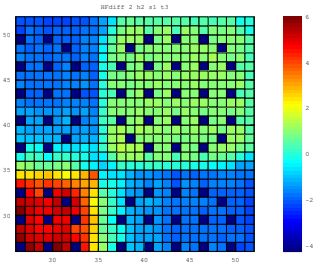

C3 M10-M30-U20

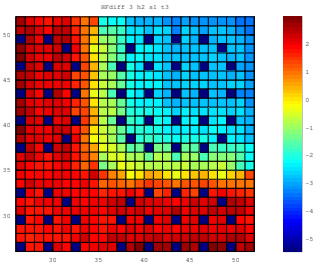

C4 M20-M50-M0

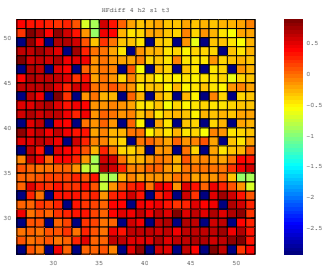

C5 M20-U20-U20

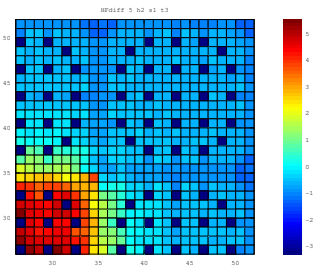

C6 U0-M30-M30

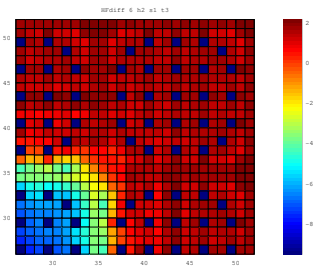

C7 M0-M0-U60

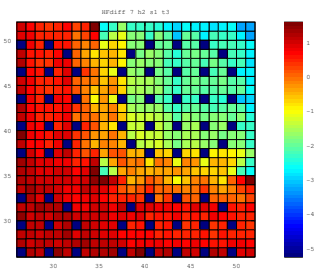

C8 M60-U10-M40

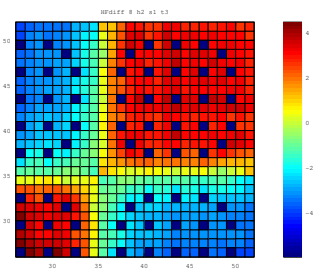

C9 U12-U12-U12

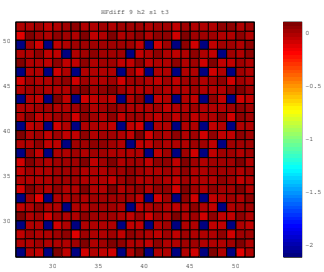

C10 U0-U36-U12

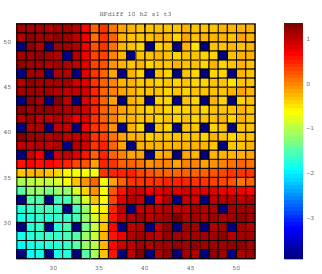

C11 M20-U0-U40

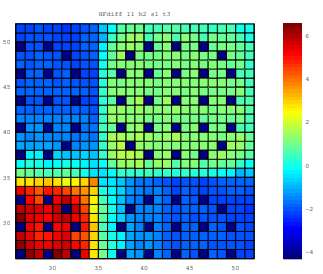

C12 M12-M12-M12

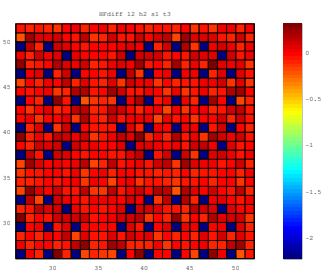

FIGURE 16 – Transport vs diffusion pin power distribution of all clusters shpnew SELE_EDF

Références

[1] M. Fliscounakis, E. Girardi and T. Courau, *A Generalized Pin-Power Reconstruction Method for Arbitrary Heterogeneous Geometries*, M&C 2011, Rio de Janero, Brasil, May 8-12 2011.

[2] C. Brosselard, H. Leroyer, M. Fliscounakis, E. Girardi and D. Couyras, *Normalization Methods for Diffusion Calculations with Various Assembly Homogenizations*, PHYSOR 2014, Kyoto, Japan, Sep. 28 - Oct. 3 2014.

[3] A. Hébert, *Applied Reactor Physics*, Presses Internationales Polytechnique, ISBN 978-2-553-01436-9, 424 p., Montréal, 2009.

[4] G. Marleau and A. Hébert, "A New Driver for Collision Probability Transport Codes", *Int. Top. Mtg. on Advances in Nuclear Engineering Computation and Radiation Shielding*, Santa Fe, New Mexico, April 9–13 (1989).

[5] G. Marleau, R. Roy and A. Hébert, "DRAGON : A Collision Probability Transport Code for Cell and Supercell Calculations", Report IGE–157, École Polytechnique de Montréal (1993).

[6] G. Marleau, A. Hébert and R. Roy, "New Computational Methods Used in the Lattice Code DRAGON", *Top Mtg. on Advances in Reactor Physics*, Charleston, SC, March 8-11 1992 ;

[7] A. Hébert, G. Marleau and R. Roy, "Application of the Lattice Code DRAGON to CANDU Analysis", *Trans. Am. Nucl. Soc.*, **72**, 335 (1995) ;

[8] A. Hébert and R. Roy, "A Programmer's Guide for the GAN Generalized Driver – FORTRAN-77 version," Report IGE-158, École Polytechnique de Montréal, Institut de Génie Nucléaire (1994).

[9] R. Roy, *The CLE-2000 Tool-Box*, Report IGE–163, Institut de génie nucléaire, École Polytechnique de Montréal, Montréal, Québec (1999).

[10] A. Hébert, D. Sekki and R. Chambon , "A User Guide for DONJON Version5", Report IGE–344, École Polytechnique de Montréal (2014).

[11] G. Marleau, A. Hébert and R. Roy , "A User Guide for DRAGON Version5", Report IGE–335, École Polytechnique de Montréal (2014).

[12] A. Hébert, G. Marleau and R. Roy , "A Description of the DRAGON and TRIVAC Version4 Data Structures", Report IGE–295, École Polytechnique de Montréal (2014).

[13] A. Hébert, "A User Guide for TRIVAC Version4", Report IGE–293, École Polytechnique de Montréal (2014).

[14] A. Hébert and G. Mathonnière, *Development of a Third-Generation Superhomogénéisation Method for the Homogenization of a Pressurized Water Reactor Assembly*, Nuc. Sci. Eng., 115, pp 129-141